High Performance and Parallel Computing
for Materials Defects and Multiphase Flows

Dynamic Rupture Earthquake Simulations on Petascale Heterogeneous Supercomputers

M. Bader, A. Breuer, S. Rettenberger,
A.-A. Gabriel, C. Pelties, A. Heinecke

Singapore, 14 Jan 2015

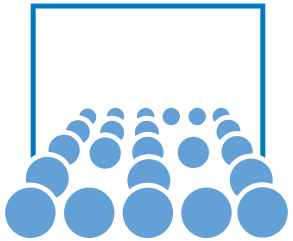

SeisSol Core Developers

Alexander Breuer

Alice-Agnes Gabriel

Alexander Heinecke

Christian Pelties

Sebastian Rettenberger

Overview and Agenda

Dynamic Rupture and Earthquake Simulation with SeisSol:

- unstructured tetrahedral meshes
- high-order ADER-DG discretisation
- target applications: earthquake dynamics, tsunami generation

Towards Scalable I/O:

- two-stage scheme to generate and read mesh partitions
- improve scalability of output and checkpointing

Optimisation for Heterogeneous Petascale Platforms:

- code generation to optimize element-local matrix kernels
- offload scheme to address multiphysics

Petascale Runs on Tianhe-2, Stampede and SuperMUC:

- weak scaling of wave propagation component
- strong scaling for 1992 Landers M7.2 earthquake

Part I

Dynamic Rupture and Earthquake Simulation with SeisSol

http://seissol.geophysik.uni-muenchen.de/

Dynamic Rupture and Earthquake Simulation

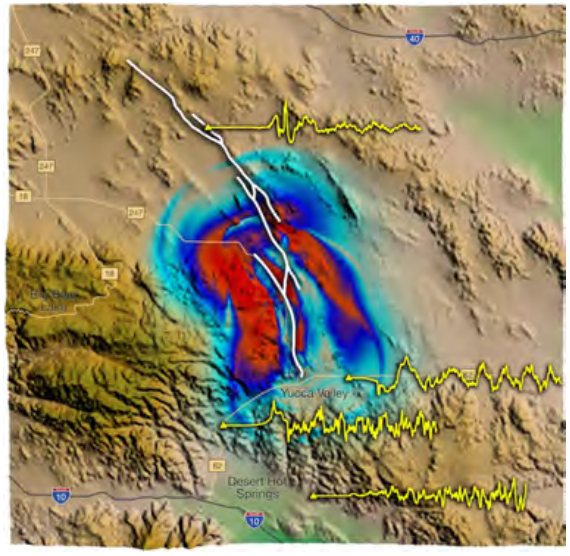

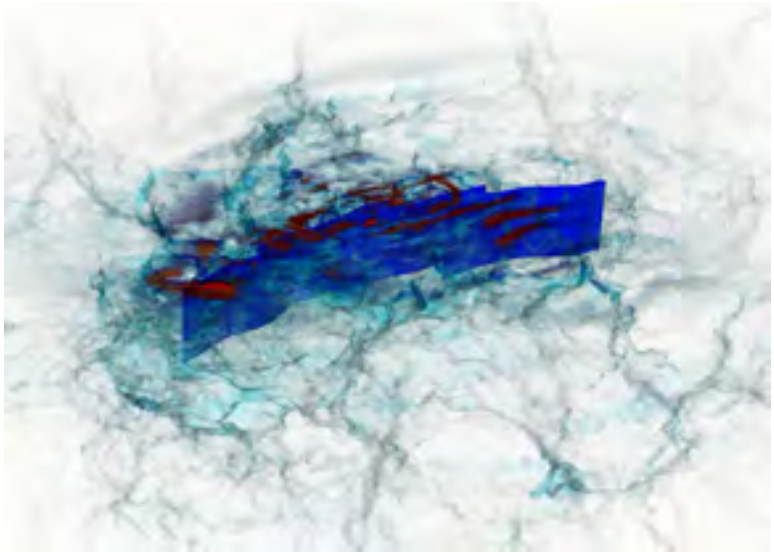

Landers fault system: simulated ground motion and seismic waves

SeisSol – ADER-DG for seismic simulations:

- adaptive tetrahedral meshes
  $\rightarrow$ complex geometries, heterogeneous media, multiphysics
- complicated fault systems with multiple branches
  $\rightarrow$ non-linear multiphysics dynamic rupture simulation
- ADER-DG: high-order discretization in space and time

1992 Landers M7.2 Earthquake

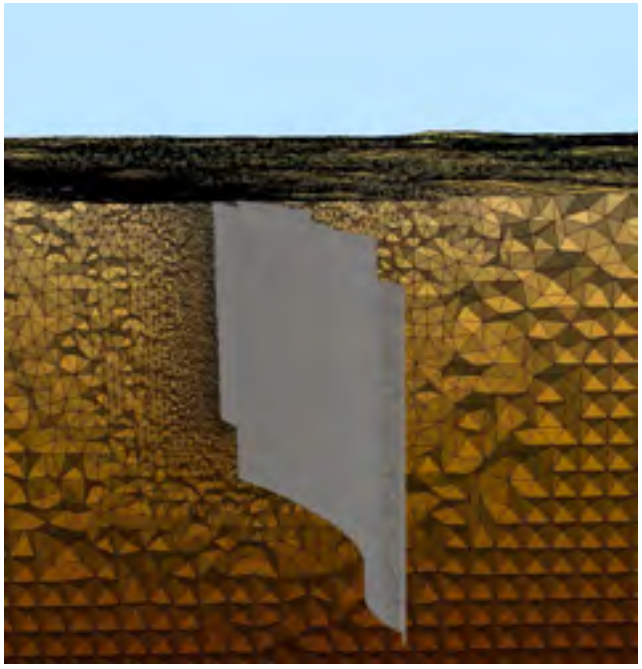

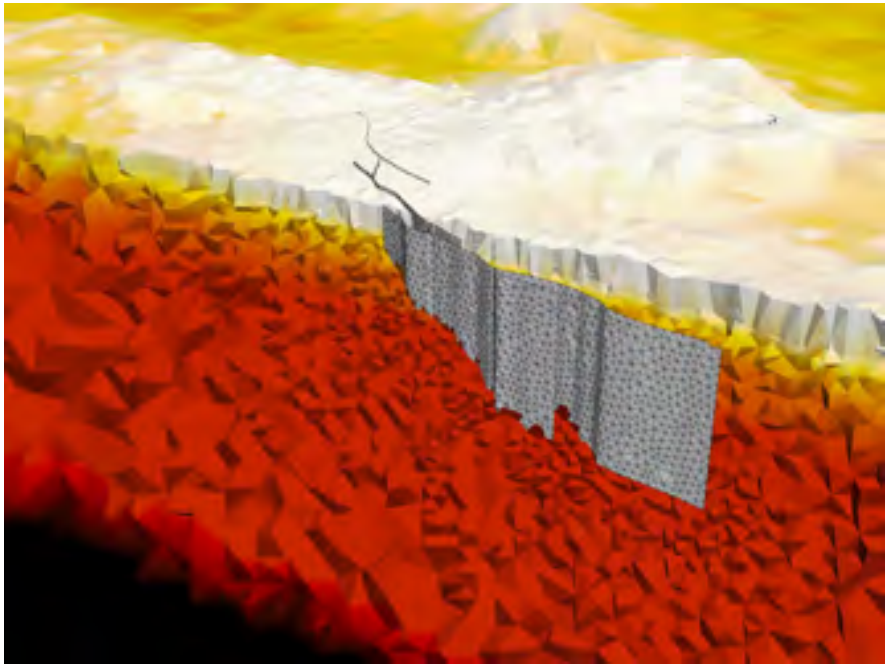

- multiphysics simulation of dynamic rupture and resulting ground motion of a M7.2 earthquake
- fault inferred from measured data, regional topography from satellite data, physically consistent stress and friction parameters
- 1D velocity structure, low velocity near surface

Multiphysics Dynamic Rupture Simulation

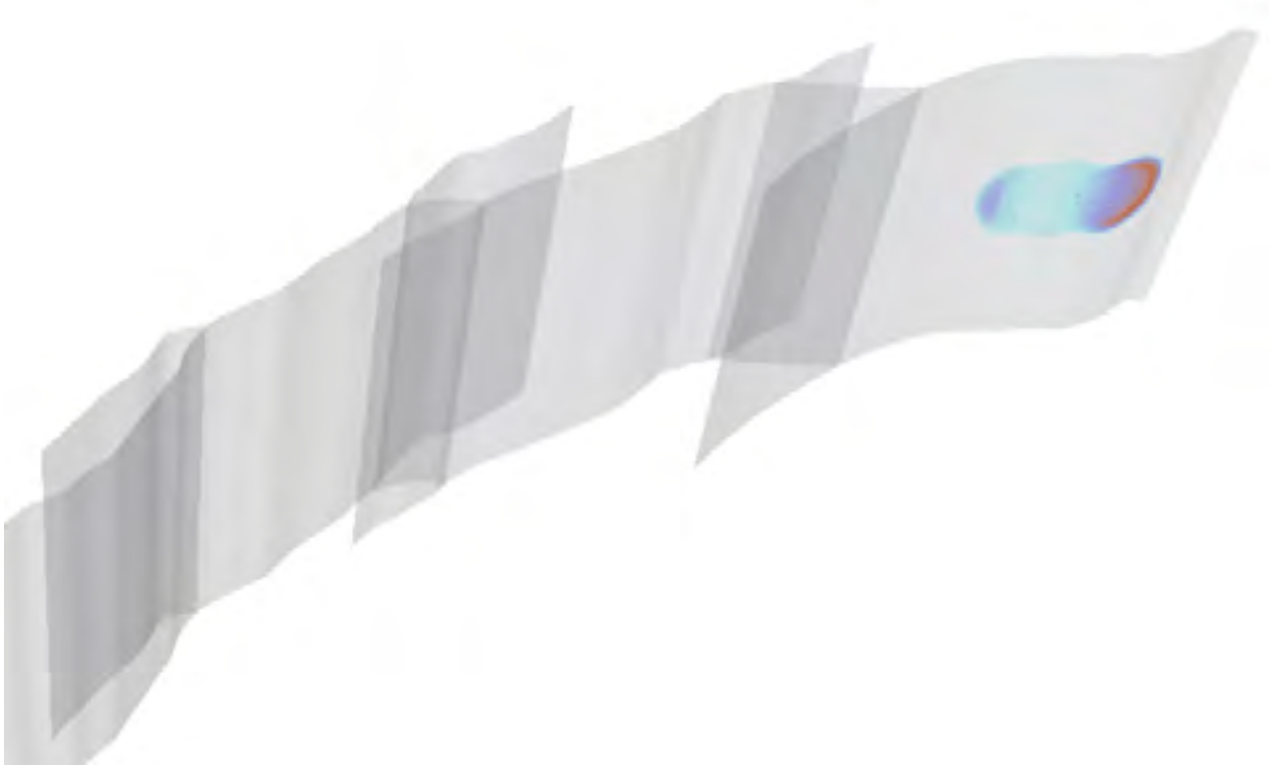

- spontaneous rupture, non-linear interaction with wave-field
- featuring rupture jumps, fault branching, etc.
- tackles fundamental questions on earthquake dynamics
- realistic rupture source for seismic hazard assessment

Multiphysics Dynamic Rupture Simulation

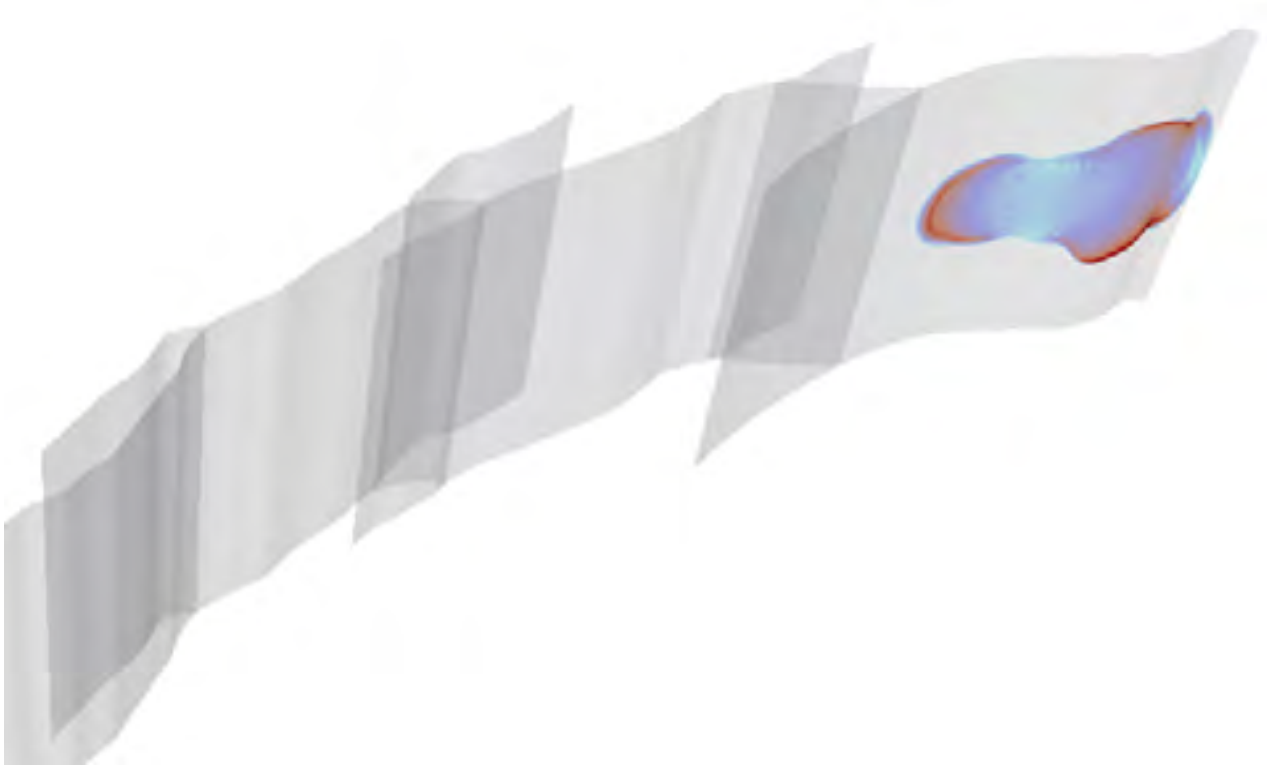

- spontaneous rupture, non-linear interaction with wave-field
- featuring rupture jumps, fault branching, etc.
- tackles fundamental questions on earthquake dynamics
- realistic rupture source for seismic hazard assessment

Multiphysics Dynamic Rupture Simulation

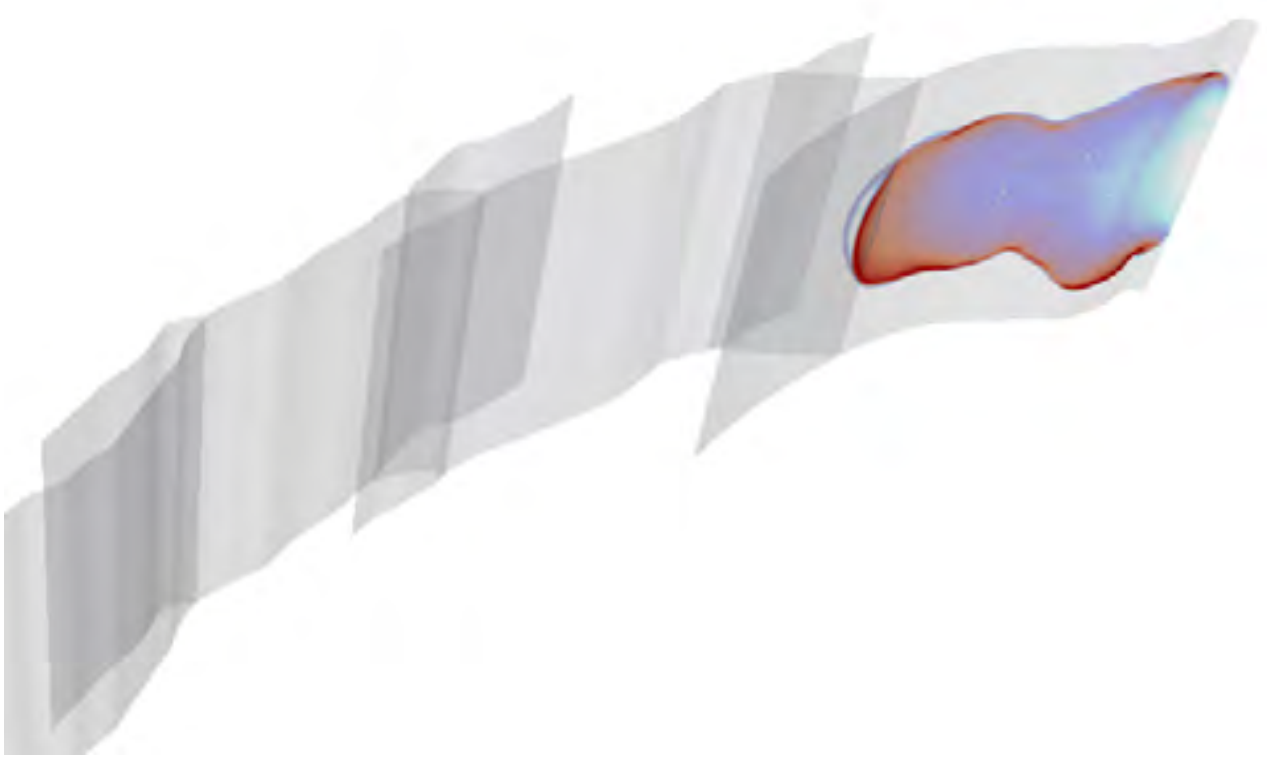

- spontaneous rupture, non-linear interaction with wave-field
- featuring rupture jumps, fault branching, etc.
- tackles fundamental questions on earthquake dynamics
- realistic rupture source for seismic hazard assessment

Multiphysics Dynamic Rupture Simulation

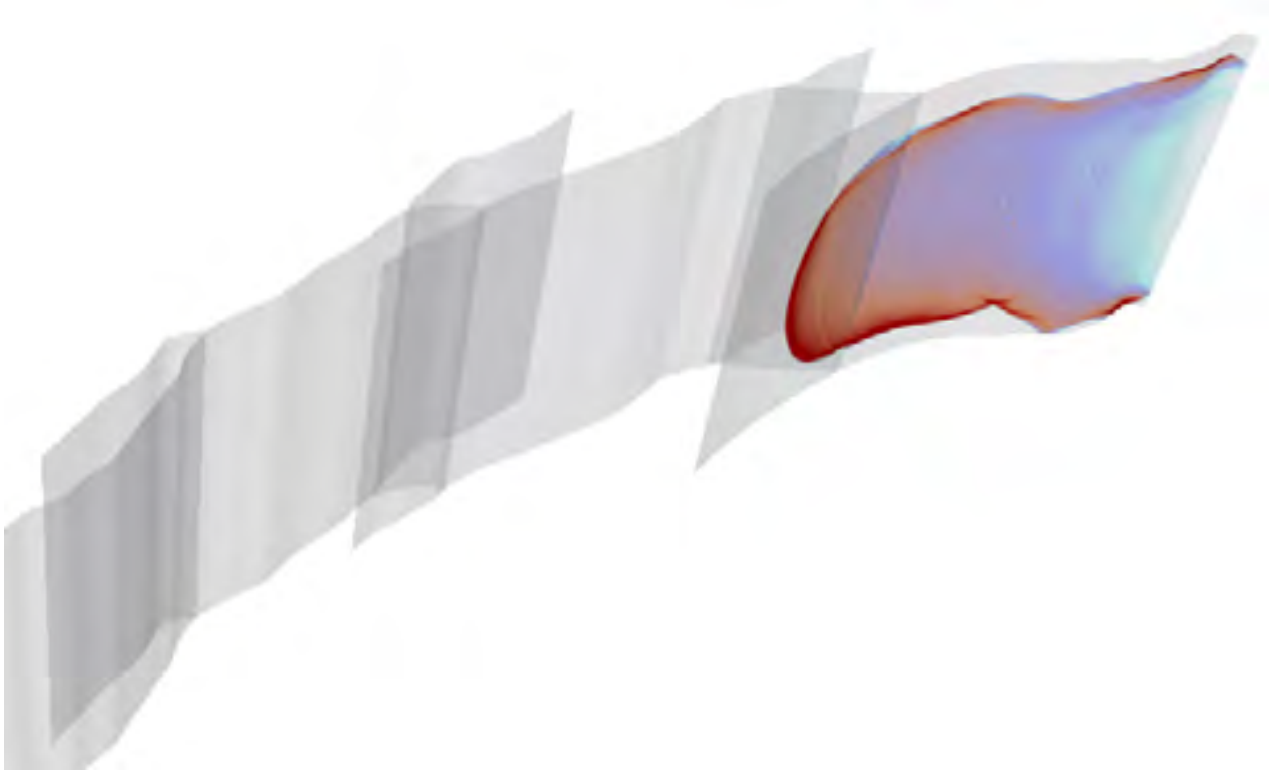

- spontaneous rupture, non-linear interaction with wave-field
- featuring rupture jumps, fault branching, etc.
- tackles fundamental questions on earthquake dynamics
- realistic rupture source for seismic hazard assessment

Multiphysics Dynamic Rupture Simulation

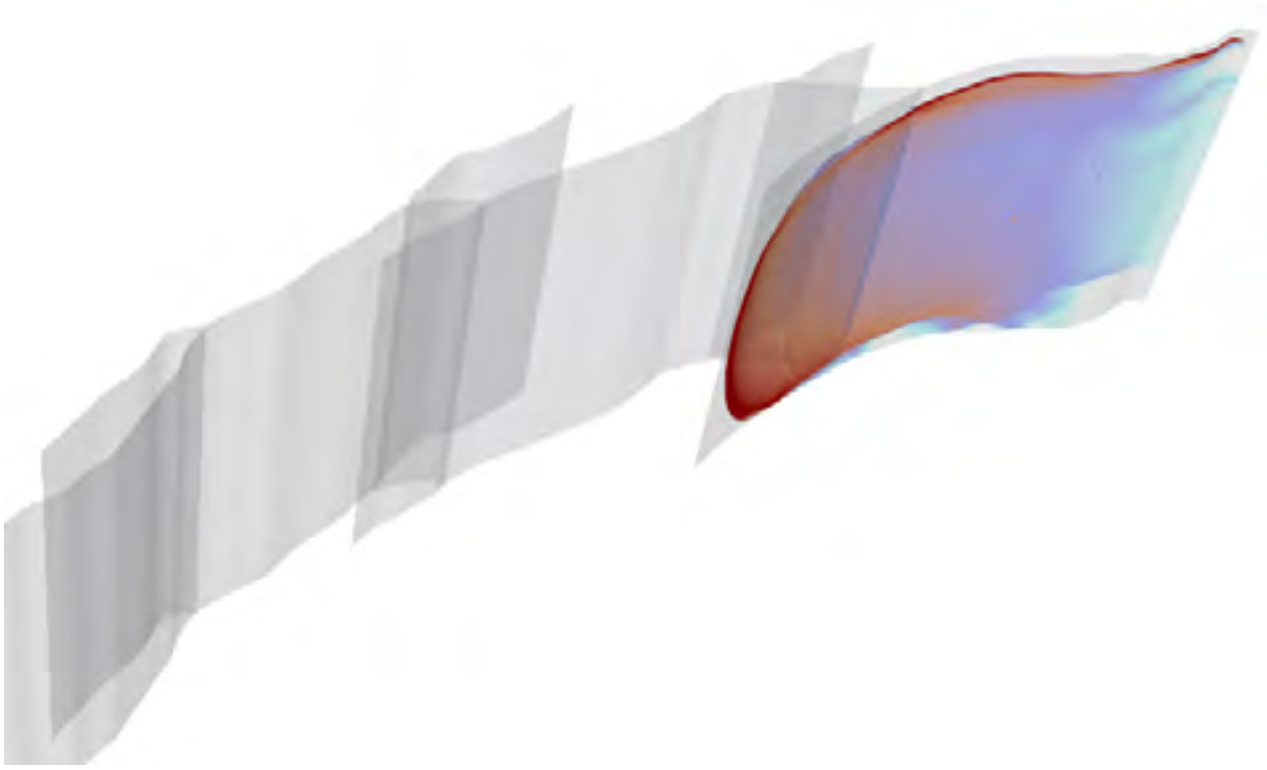

- spontaneous rupture, non-linear interaction with wave-field
- featuring rupture jumps, fault branching, etc.
- tackles fundamental questions on earthquake dynamics
- realistic rupture source for seismic hazard assessment

Multiphysics Dynamic Rupture Simulation

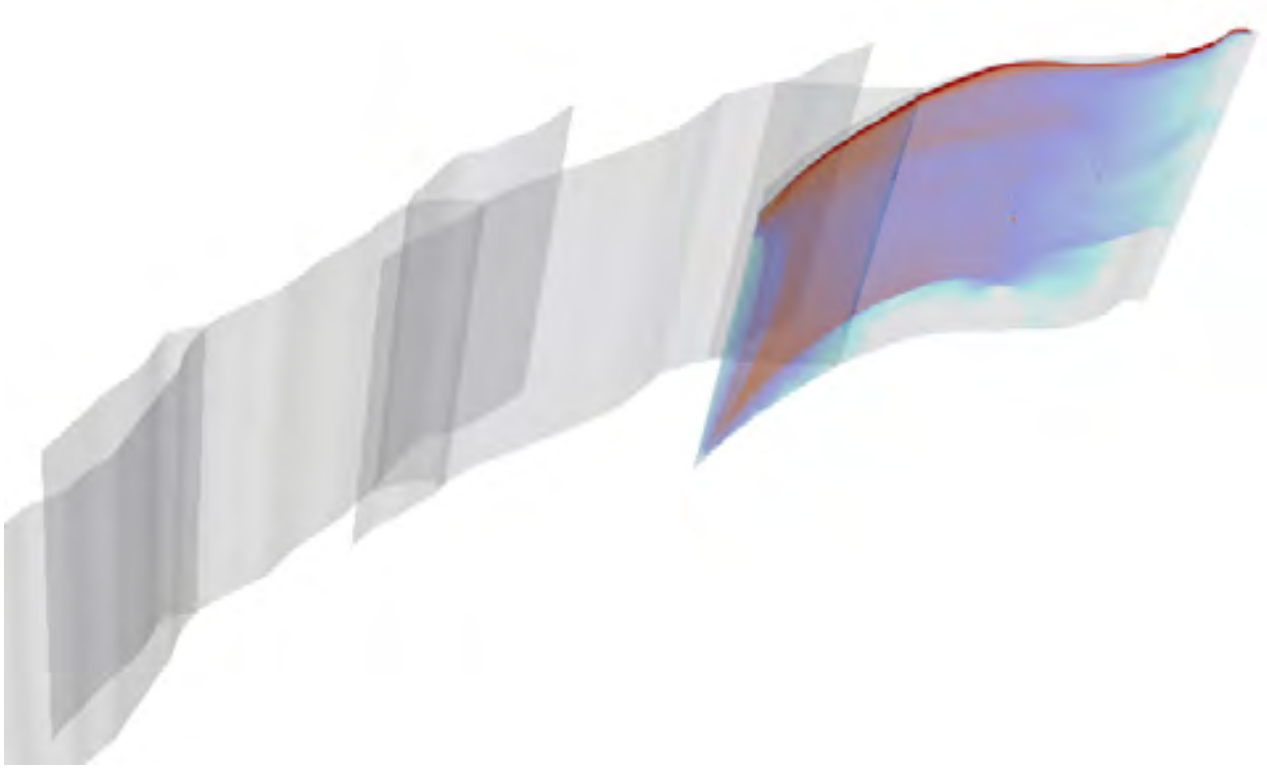

- spontaneous rupture, non-linear interaction with wave-field
- featuring rupture jumps, fault branching, etc.
- tackles fundamental questions on earthquake dynamics
- realistic rupture source for seismic hazard assessment

Multiphysics Dynamic Rupture Simulation

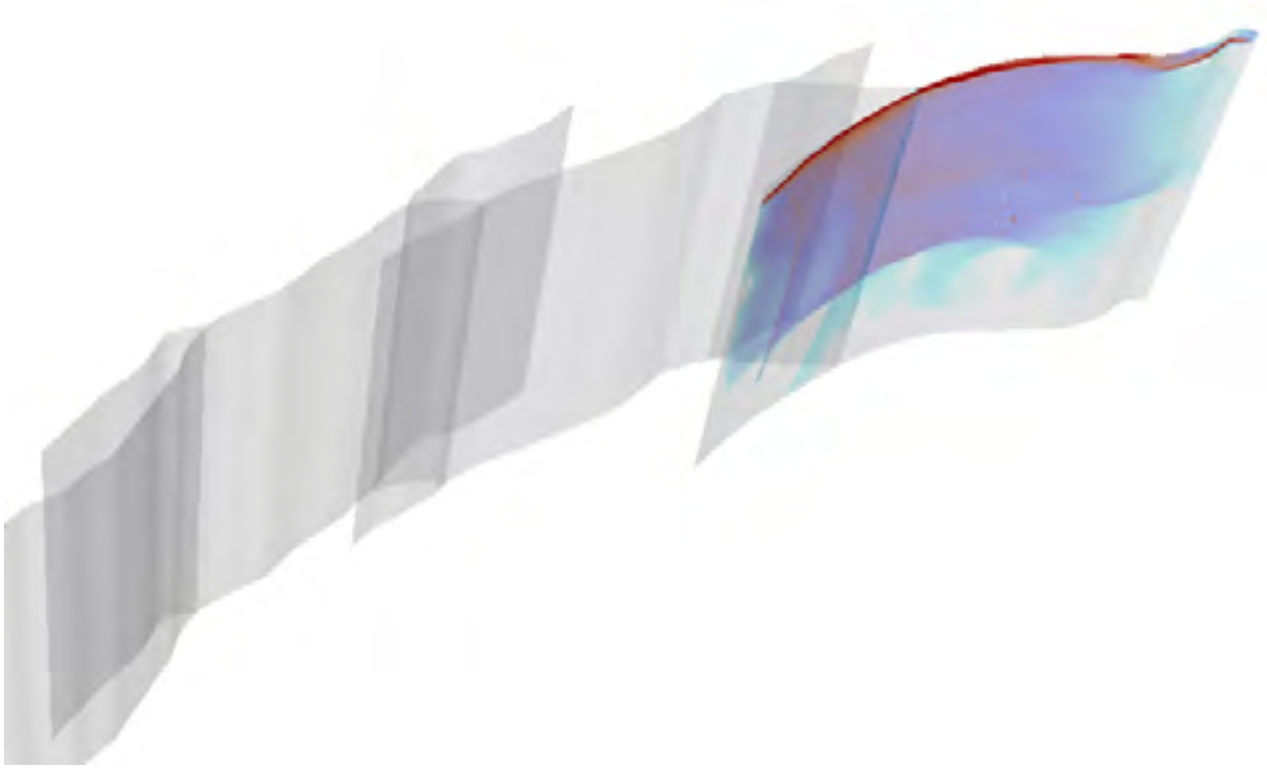

- spontaneous rupture, non-linear interaction with wave-field
- featuring rupture jumps, fault branching, etc.
- tackles fundamental questions on earthquake dynamics
- realistic rupture source for seismic hazard assessment

Multiphysics Dynamic Rupture Simulation

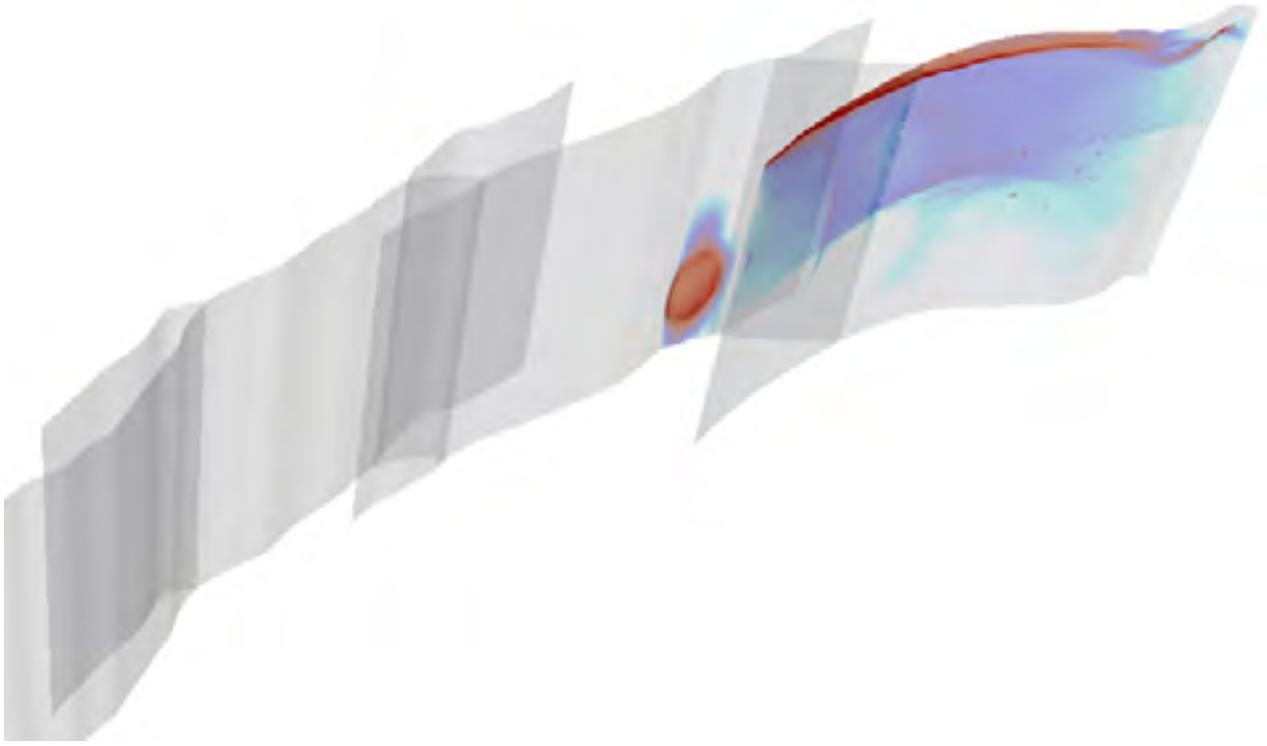

- spontaneous rupture, non-linear interaction with wave-field
- featuring rupture jumps, fault branching, etc.
- tackles fundamental questions on earthquake dynamics
- realistic rupture source for seismic hazard assessment

Multiphysics Dynamic Rupture Simulation

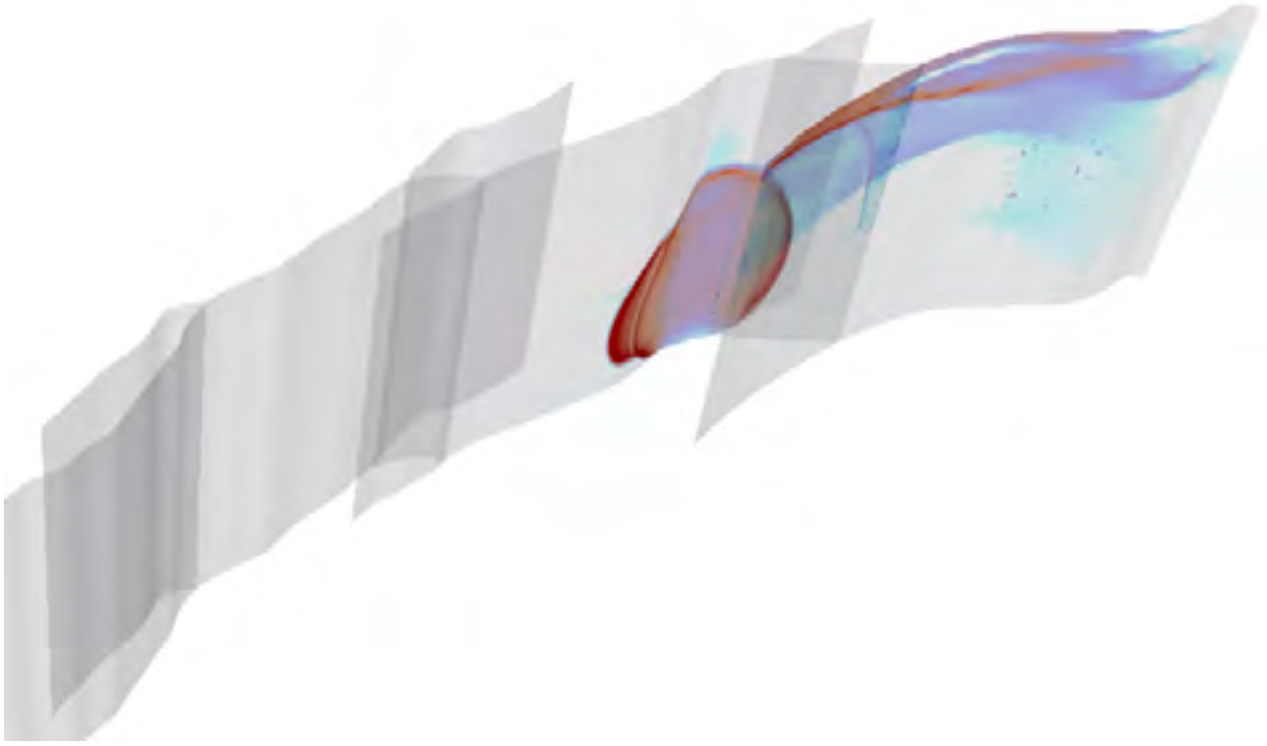

- spontaneous rupture, non-linear interaction with wave-field
- featuring rupture jumps, fault branching, etc.
- tackles fundamental questions on earthquake dynamics
- realistic rupture source for seismic hazard assessment

Multiphysics Dynamic Rupture Simulation

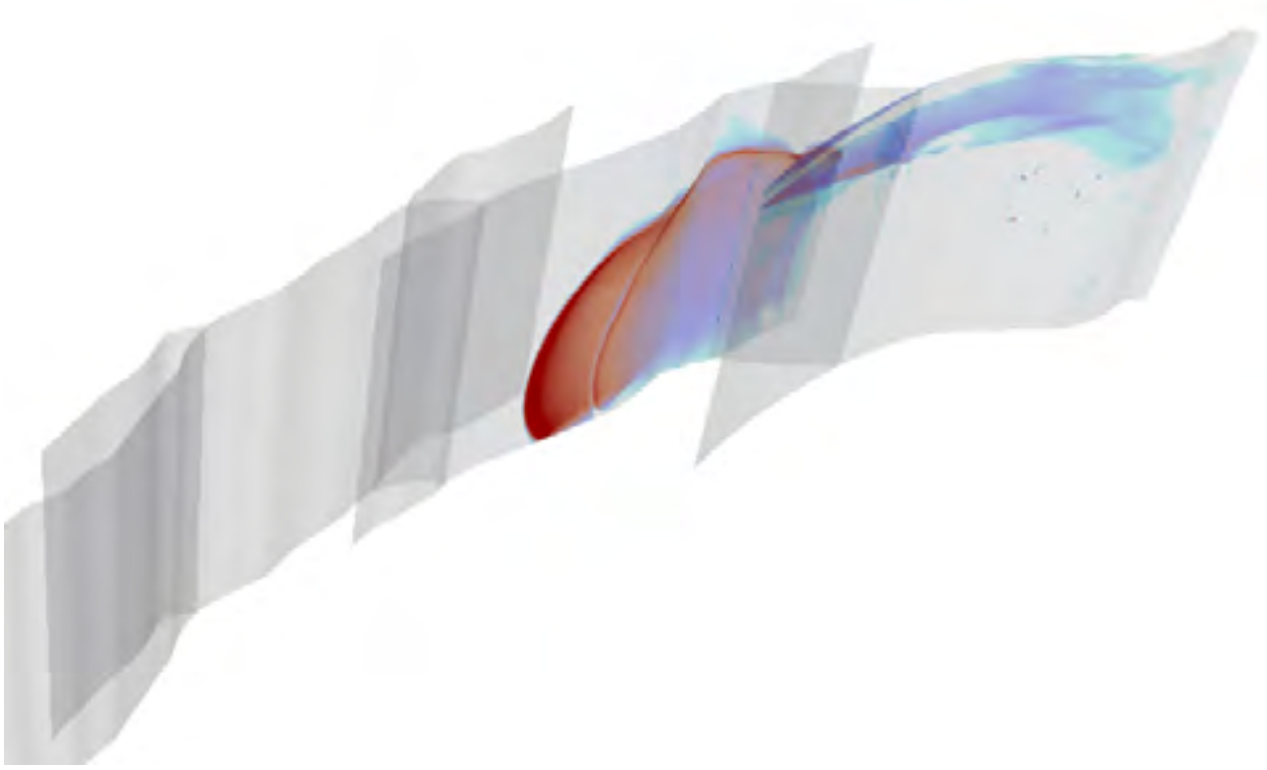

- spontaneous rupture, non-linear interaction with wave-field
- featuring rupture jumps, fault branching, etc.
- tackles fundamental questions on earthquake dynamics
- realistic rupture source for seismic hazard assessment

Multiphysics Dynamic Rupture Simulation

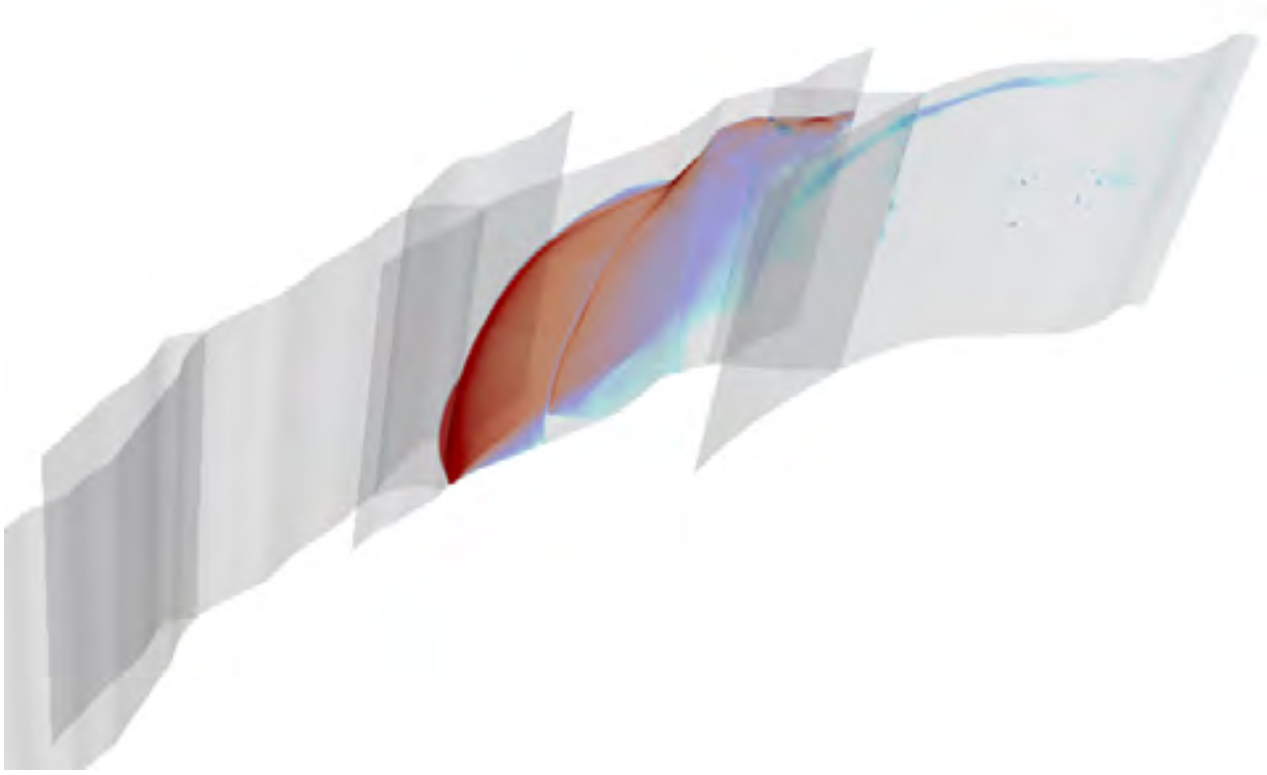

- spontaneous rupture, non-linear interaction with wave-field
- featuring rupture jumps, fault branching, etc.
- tackles fundamental questions on earthquake dynamics
- realistic rupture source for seismic hazard assessment

Multiphysics Dynamic Rupture Simulation

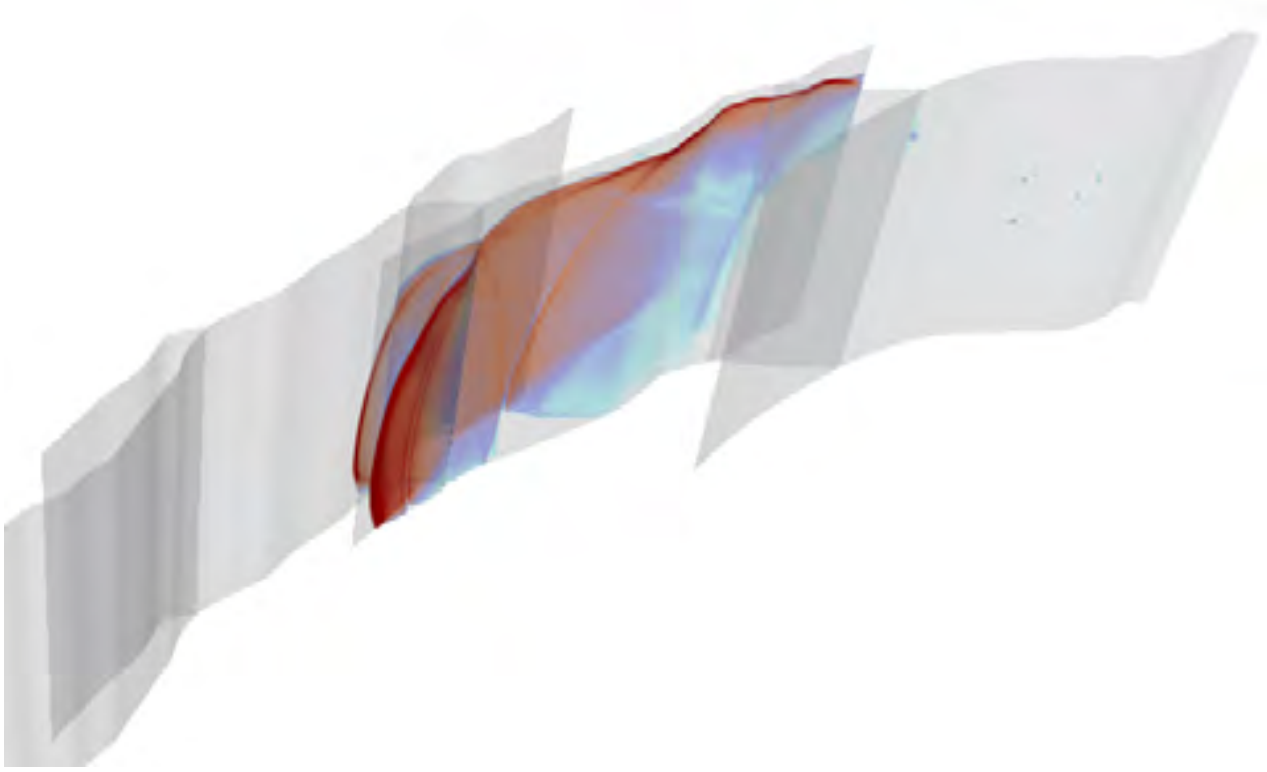

- spontaneous rupture, non-linear interaction with wave-field
- featuring rupture jumps, fault branching, etc.
- tackles fundamental questions on earthquake dynamics
- realistic rupture source for seismic hazard assessment

Multiphysics Dynamic Rupture Simulation

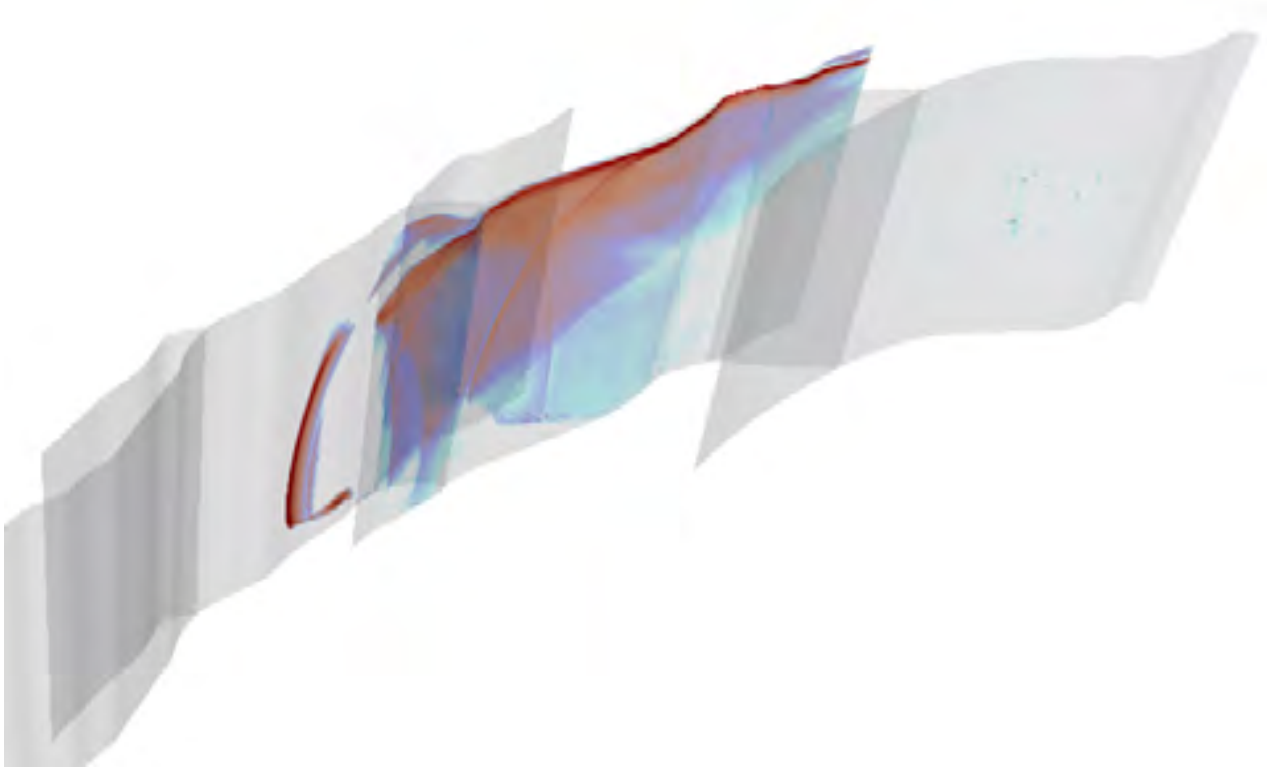

- spontaneous rupture, non-linear interaction with wave-field
- featuring rupture jumps, fault branching, etc.
- tackles fundamental questions on earthquake dynamics
- realistic rupture source for seismic hazard assessment

Multiphysics Dynamic Rupture Simulation

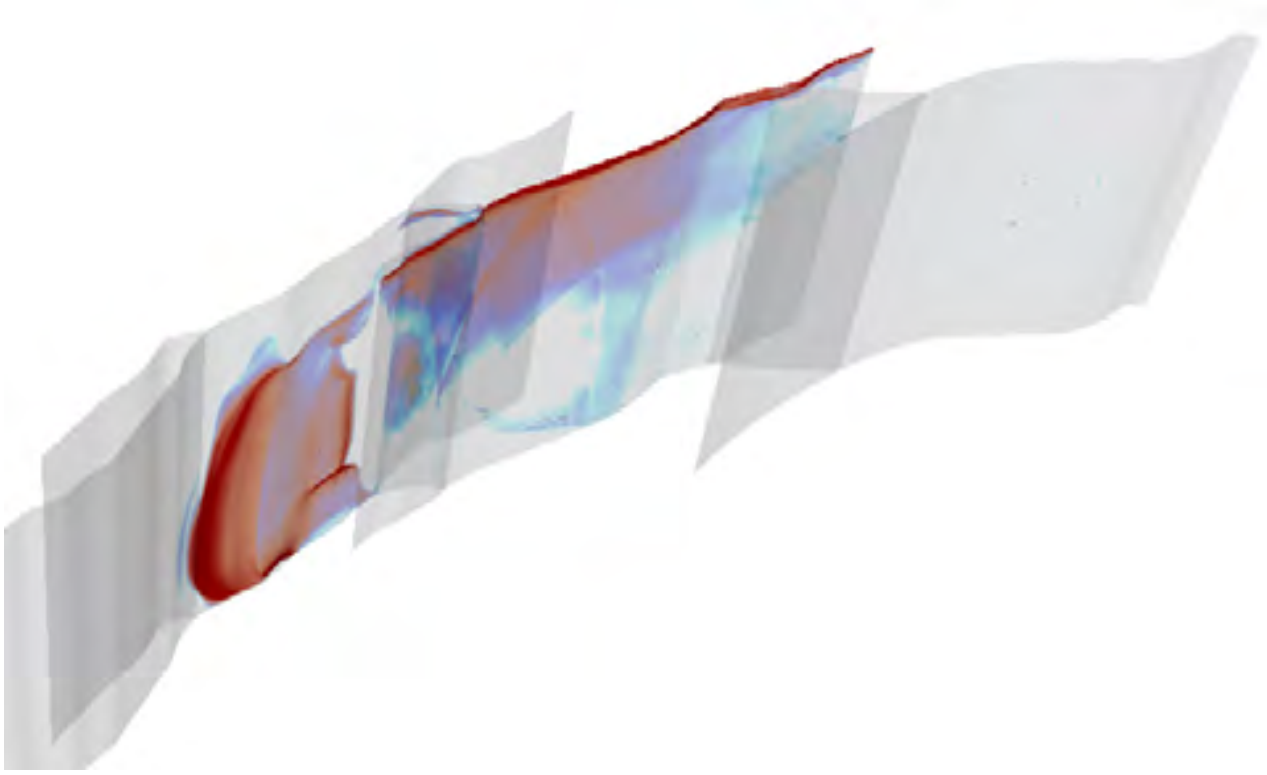

- spontaneous rupture, non-linear interaction with wave-field
- featuring rupture jumps, fault branching, etc.
- tackles fundamental questions on earthquake dynamics
- realistic rupture source for seismic hazard assessment

Multiphysics Dynamic Rupture Simulation

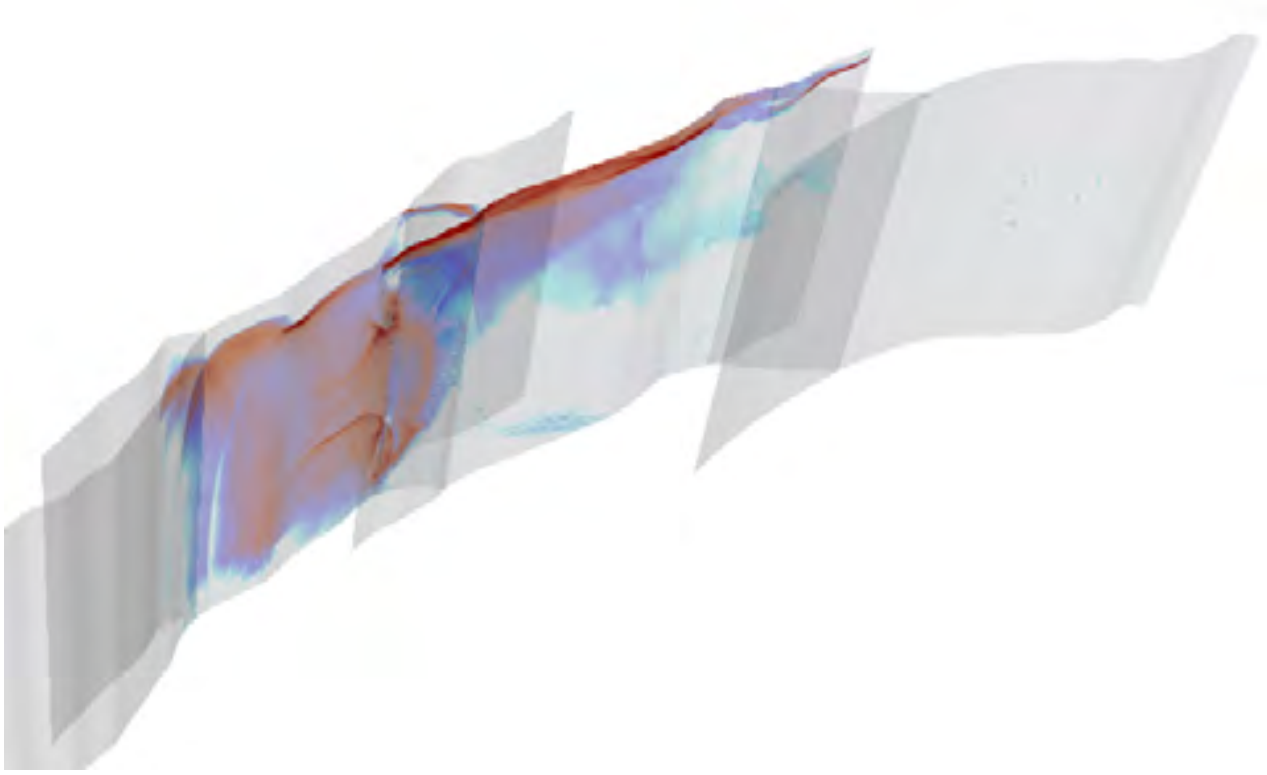

- spontaneous rupture, non-linear interaction with wave-field
- featuring rupture jumps, fault branching, etc.
- tackles fundamental questions on earthquake dynamics
- realistic rupture source for seismic hazard assessment

Landers Earthquake – Results

Observations:

- complex rupture dynamics (fault branching, etc.)
- high-frequency signals from rupture propagate directly into wave field
- synthetic seismograms with frequencies up to 10 Hz
- ground shaking in the engineering frequency band
- 42 s simulated time

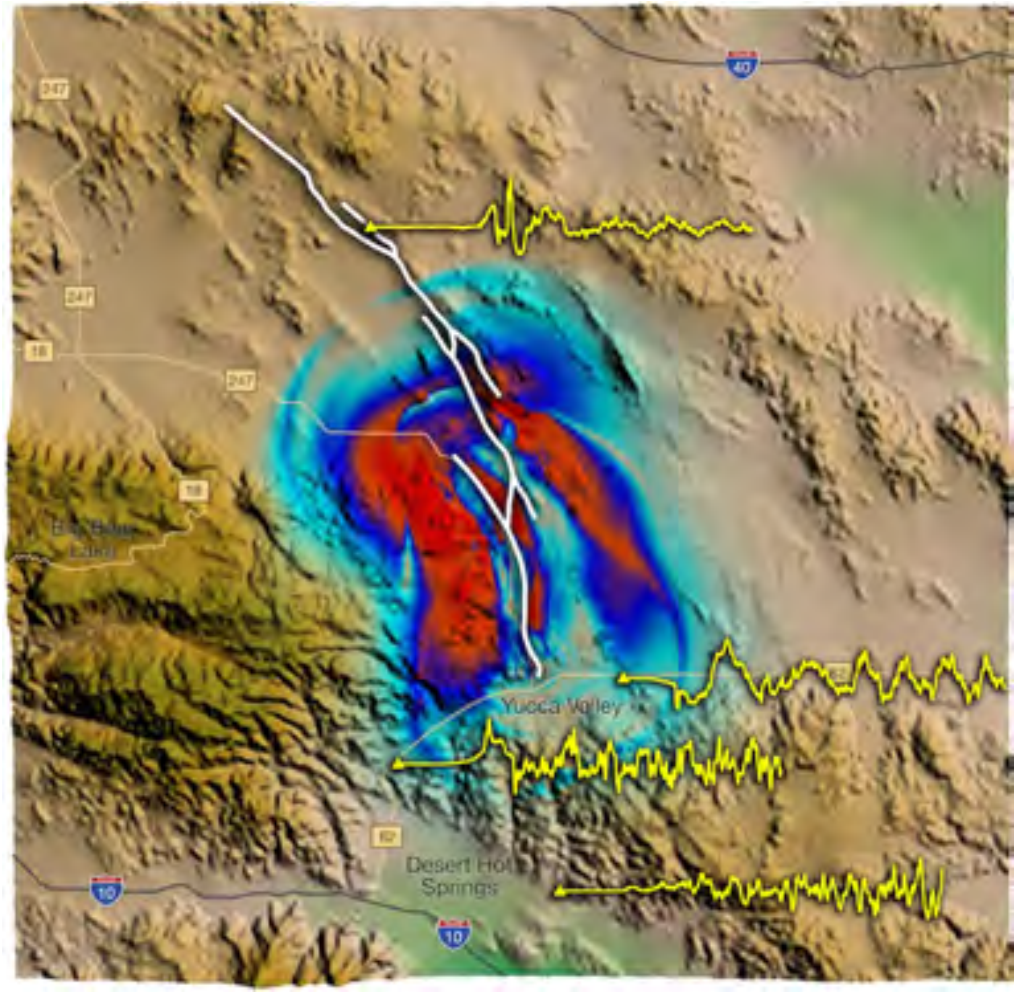

SuperMUC Production Run:

- **1.25 PFLOPS** sustained performance
- 7 h 15 min computing time

Project ASCETE

Simulation of Coupled Earthquake-Tsunami Events

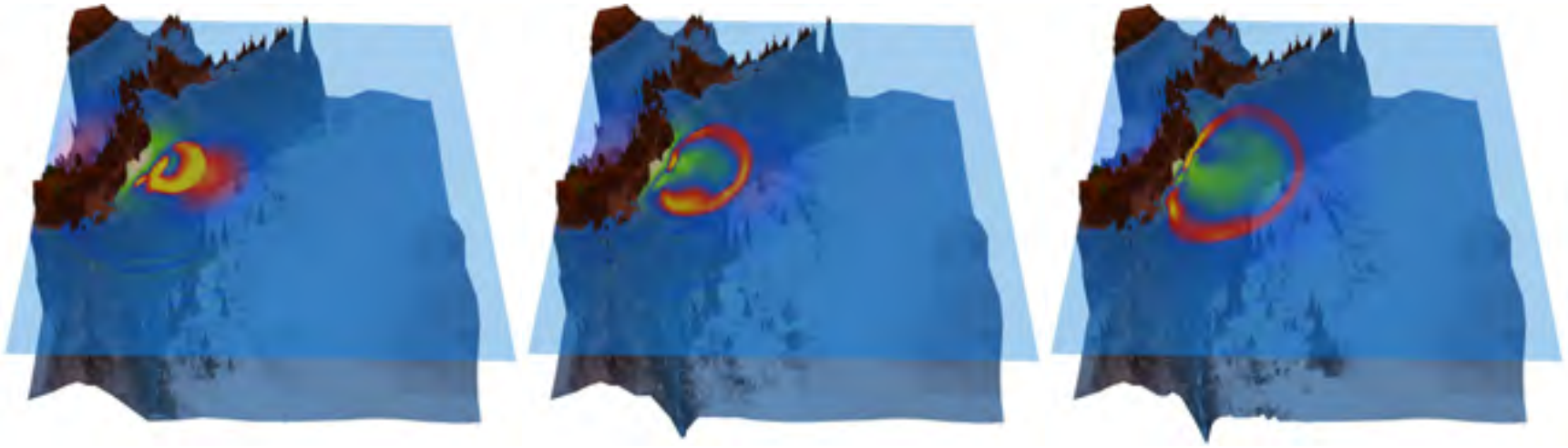

prototype simulation by P. Galvez [5] and K. Rahnema

Project Partners:

- earthquake simulation: C. Pelties, A. Gabriel, H. Igel (LMU Munich, **SeisSol**)
- seismology: L. Dalguer, P. Galvez (ETH Zürich)
- tsunami simulation: J. Behrens, S. Vater (Klima Campus, Univ. Hamburg)
- HPC: M. Bader, A. Breuer, K. Rahnema (TUM)

Simulation of Tsunamigenic Earthquakes

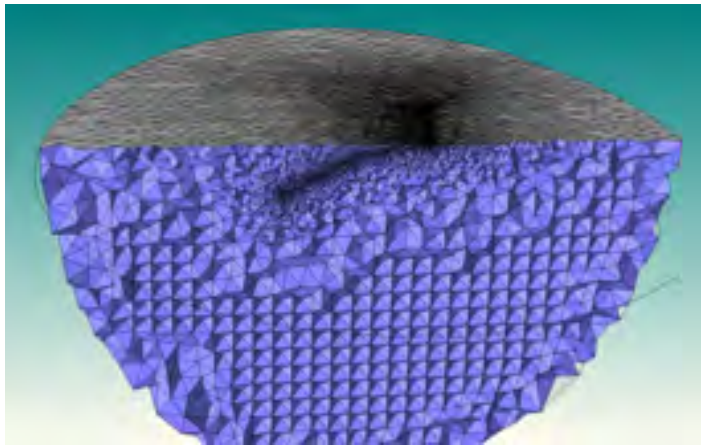

Tohoku subduction zone: CAD model and tetrahedral mesh (C. Pelties)

Challenges:

- curved subduction zones that meet surface at shallow angles
  $\rightarrow$ high impact on uplift for tsunamigenic earthquakes
- impact of time-dependent earthquake source on tsunami
  $\rightarrow$ near-field tsunami with long rupture process (Sumatra 2004)
  $\rightarrow$ near-field tsunami “double-slip” earthquake (Tohoku 2011)
- turning oceanic ground motion into shallow-water displacements

Part II

Scalable Meshing and I/O

Rettenberger, Smith, Pelties: *Parallel Unstructured Mesh Generation for the Petascale Application SeisSol*, poster, SC14.

Mesh Generation and Partitioning

Mesh Generation:

- high-quality meshes required (complicated fault structures, controllable mesh coarsening)
- with 10^8–10^9 grid cells
- using **SimModeler** by Simmetrix (`http://simmetrix.com/`)

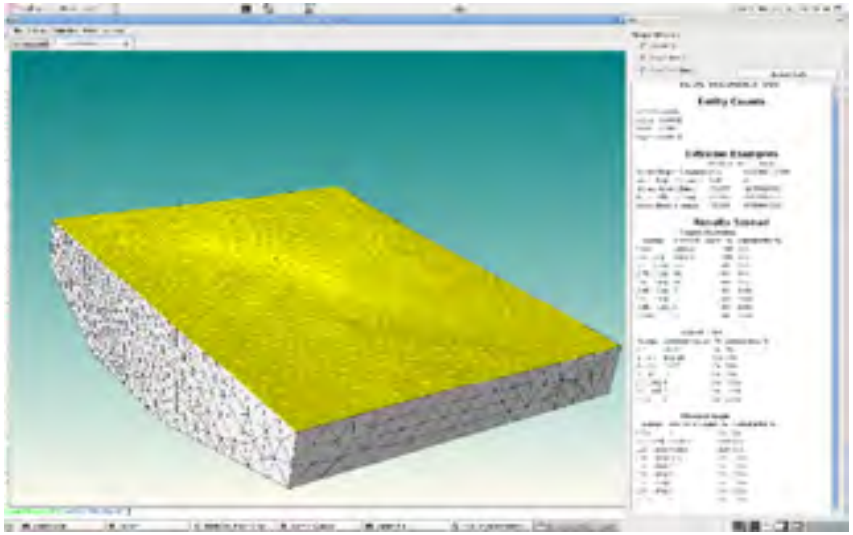

Wanted: scalable solution to provide parallel mesh partitions

- graph-based partitioning (ParMETIS)
- create customised parallel format (based on netCDF) for mesh partitions (also contains information on neighbour partitions, etc.)
- highly scalable mesh input via netCDF/MPI-IO in SeisSol

Stating Point: Init Mesh Partitions in SeisSol

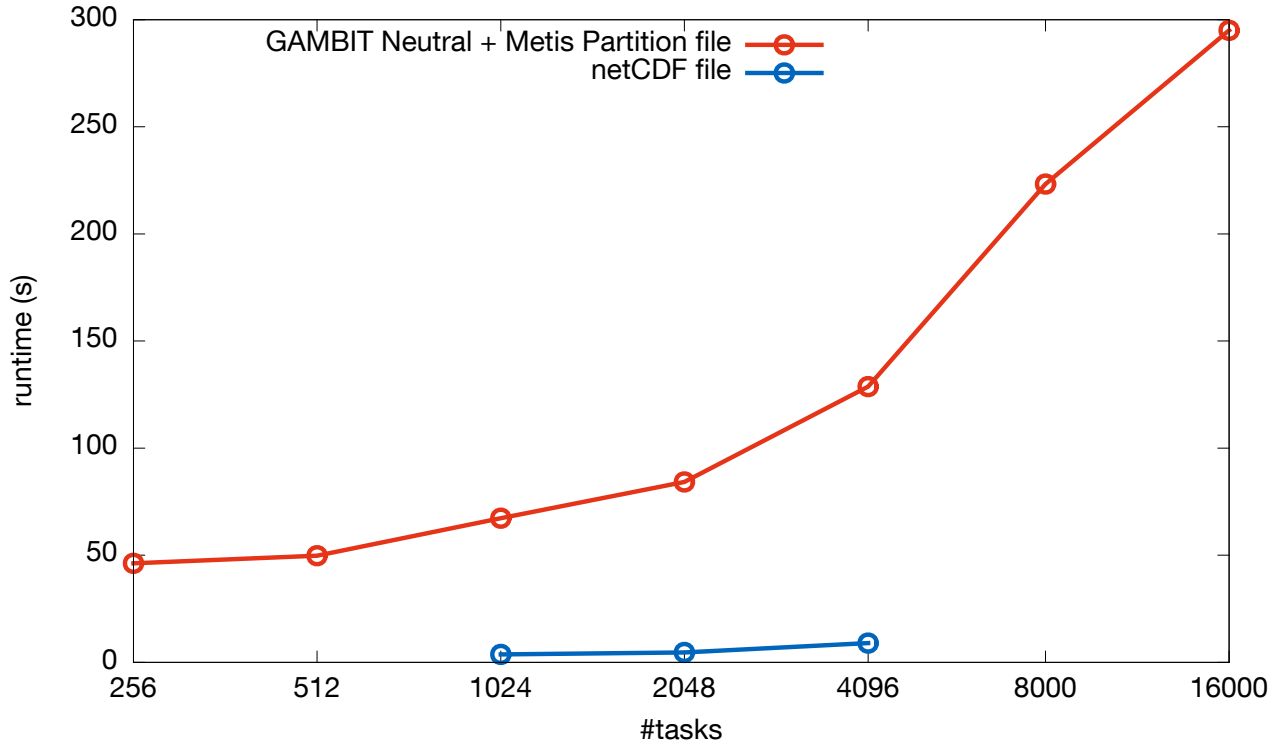

- strong scaling test on SuperMUC
- LOH.1 benchmark with 7,252,482 grid cells
- combine info from GAMBIT Neutral file and Metis Partition file
- does not scale, memory requirements per task: $O(\#cells)$

Two-stage Approach for Scalable Mesh Input

PUMgen: offline partitioning and mesh file generation

- start from mesh file as input
- call ParMETIS to compute partitions and communication structure
- write parallel mesh input file (based on netCDF format)

Resulting Mesh Pipeline:

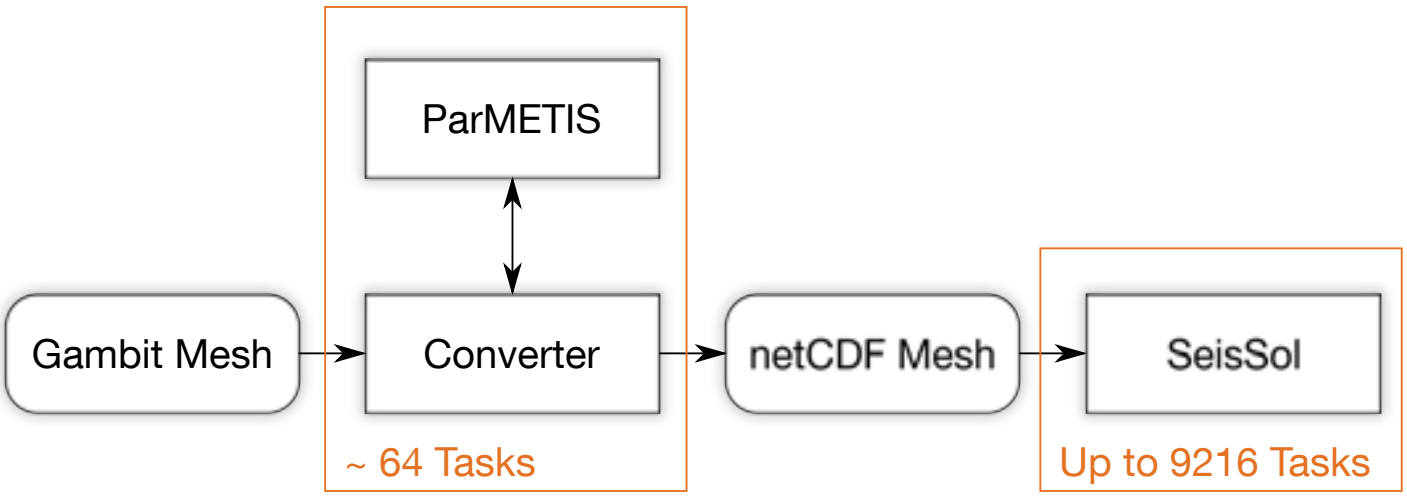

Runtime:	47.8 min	5.8 sec

Two-stage Approach for Scalable Mesh Input (2)

PUMgen: offline parallel meshing and partitioning

- start from CAD file as input
- parallel mesh generation via Simmetrix interface
- compute partitions and communication structure (ParMETIS)
- write parallel mesh input file (based on netCDF format)

Final Mesh Pipeline using PUMgen:

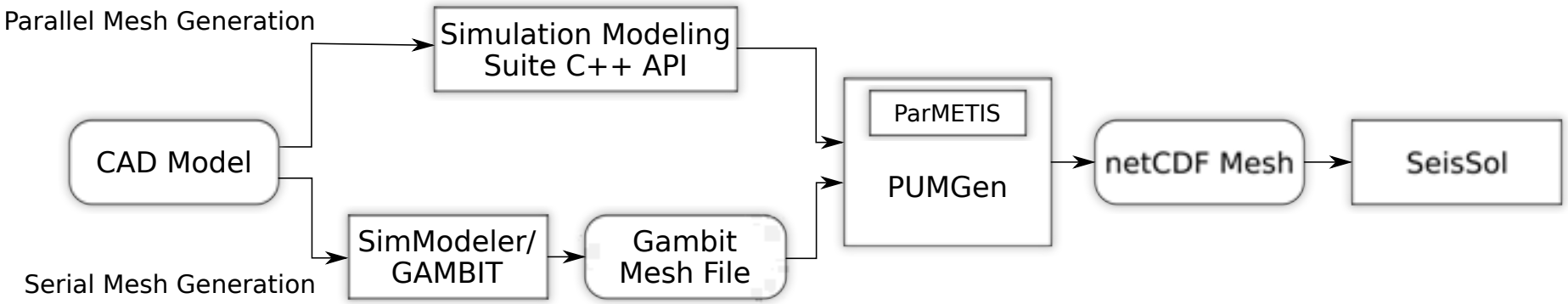

Parallel Mesh Input

- mesh and partition information combined in a single mesh file (binary file format: HDF5/netCDF)
- includes information on neighbour partitions
- includes information on partition boundaries (ghost layers, etc.)
- relies purely on collective MPI I/O operations to access data
- each processor only reads its own partition

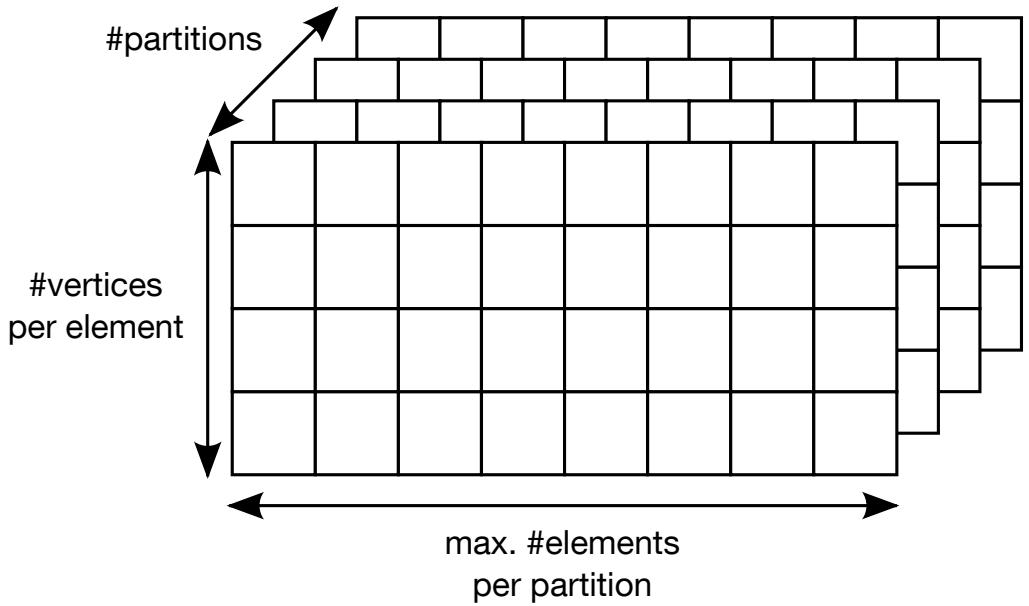

Parallel Mesh Format – Strong Scaling

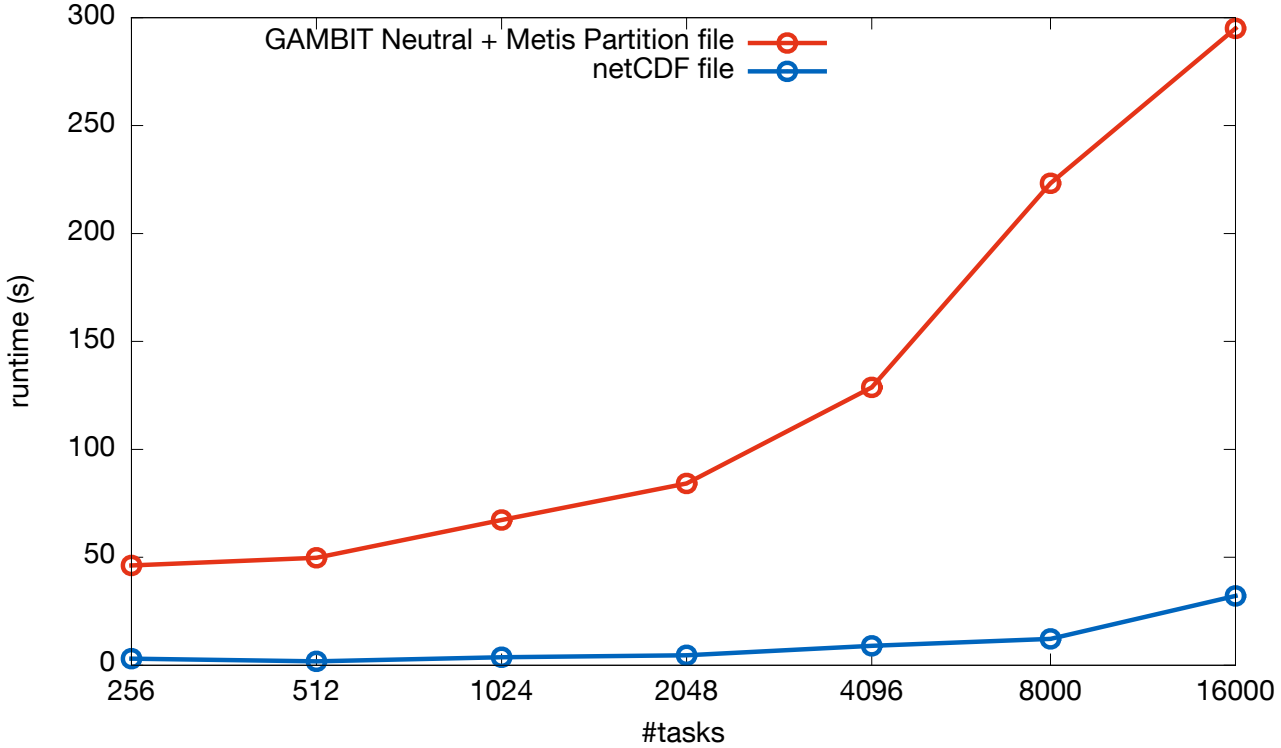

- SuperMUC
- Strong scaling
- LOH.1
- 7,252,482 cells

- Runtime and memory requirements are reduced to $O(\#cells/\#partitions)$
- largest test: mesh with 8,847,360,000 tetrahedrons read in 23 seconds on 9216 nodes/ranks

Parallel Mesh Format – Weak Scaling

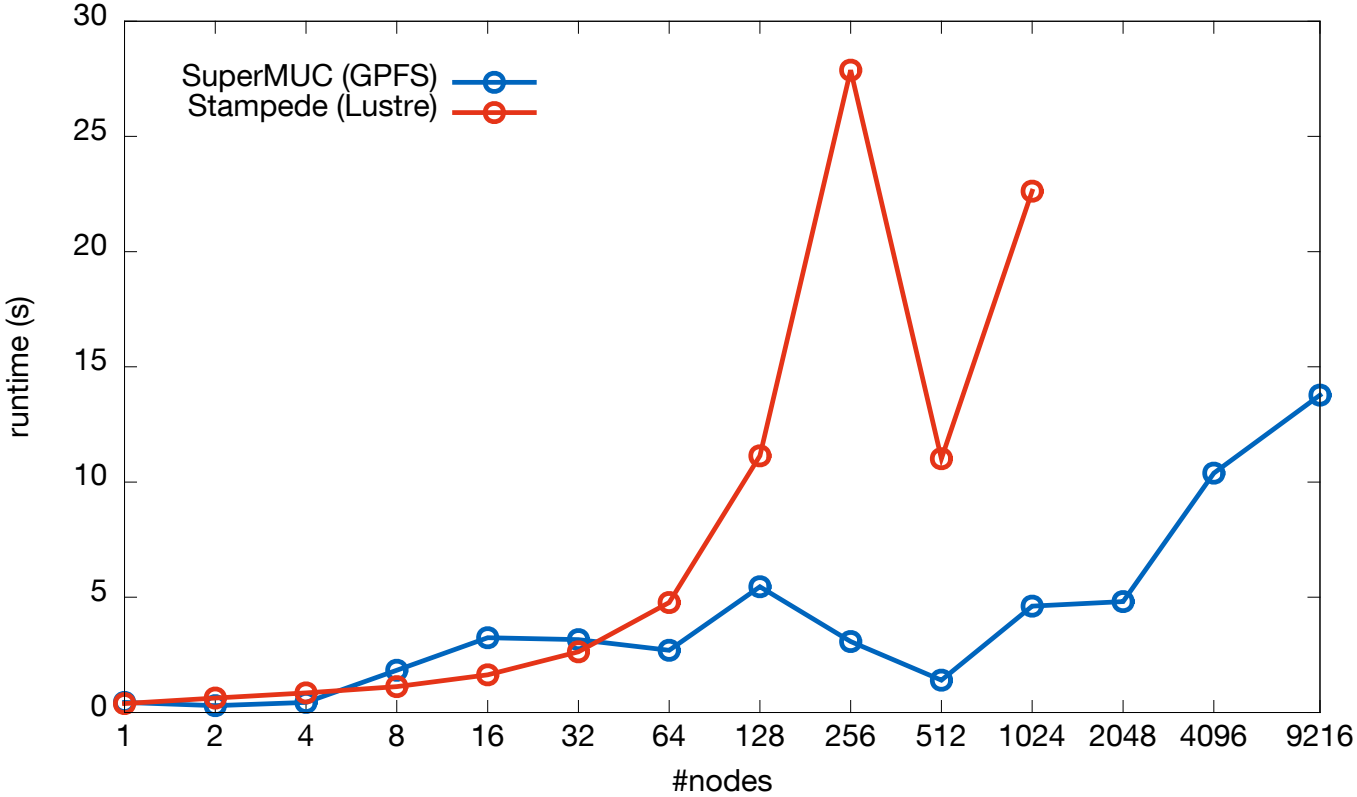

- Cubic domain, uniformly refined tetrahedral cells
- Weak scaling: 400,000 elements per node
- Largest mesh: $>$ 3.5 billion cells

Parallel Mesh Format – Weak Scaling

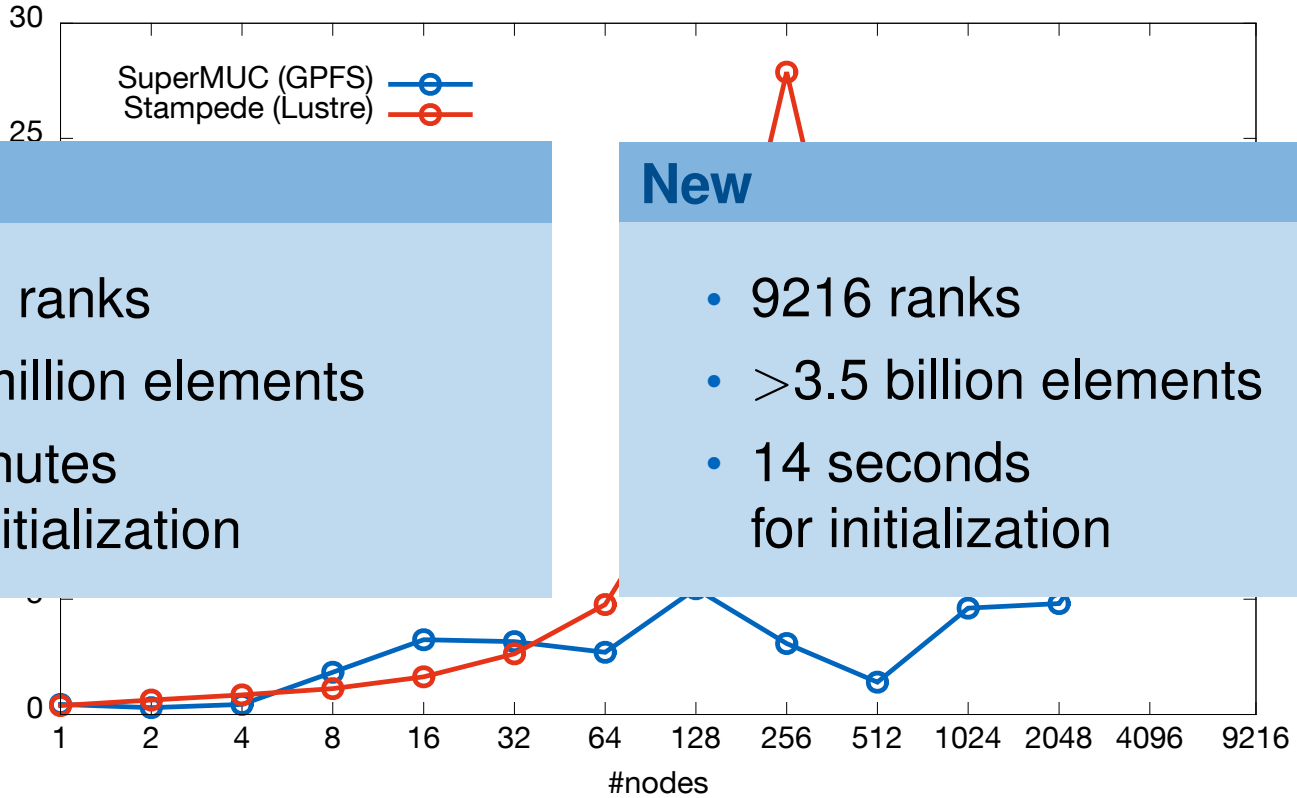

Old

- 8000 ranks
- 7.3 million elements
- 4 minutes for initialization

New

- 9216 ranks
- $>$3.5 billion elements
- 14 seconds for initialization

- Cubic domain, uniformly refined tetrahedral cells
- Weak scaling: 400,000 elements per node
- Largest mesh: $>$ 3.5 billion cells

Wave Field Visualization for SeisSol

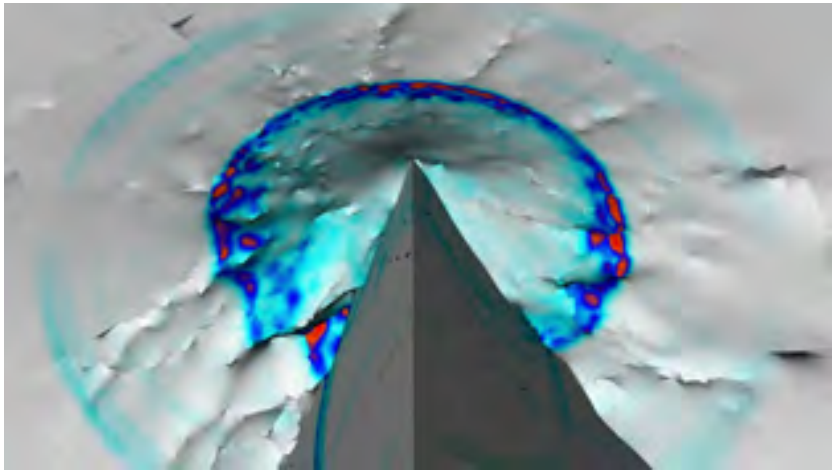

Volcano Mount Merapi

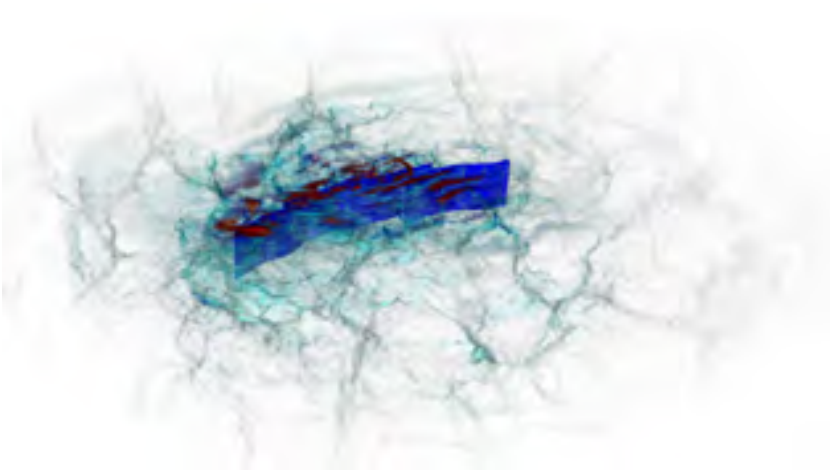

1992 Landers Earthquake

- only low-order data visualised
  $\Rightarrow$ data sets are small (compared to computational cost)
- goal: aggregate all data into a single file
  $\Rightarrow$ avoids creation of many small files & directory structures
- use **XDMF**: eXtensible Data Model and Format
  (supported by Paraview and Visit, `http://xdmf.org/`)

Writing to a Single File in Parallel

- Files can be partially locked by a process
- “Parts” are defined by the file system blocksize (GPFS)

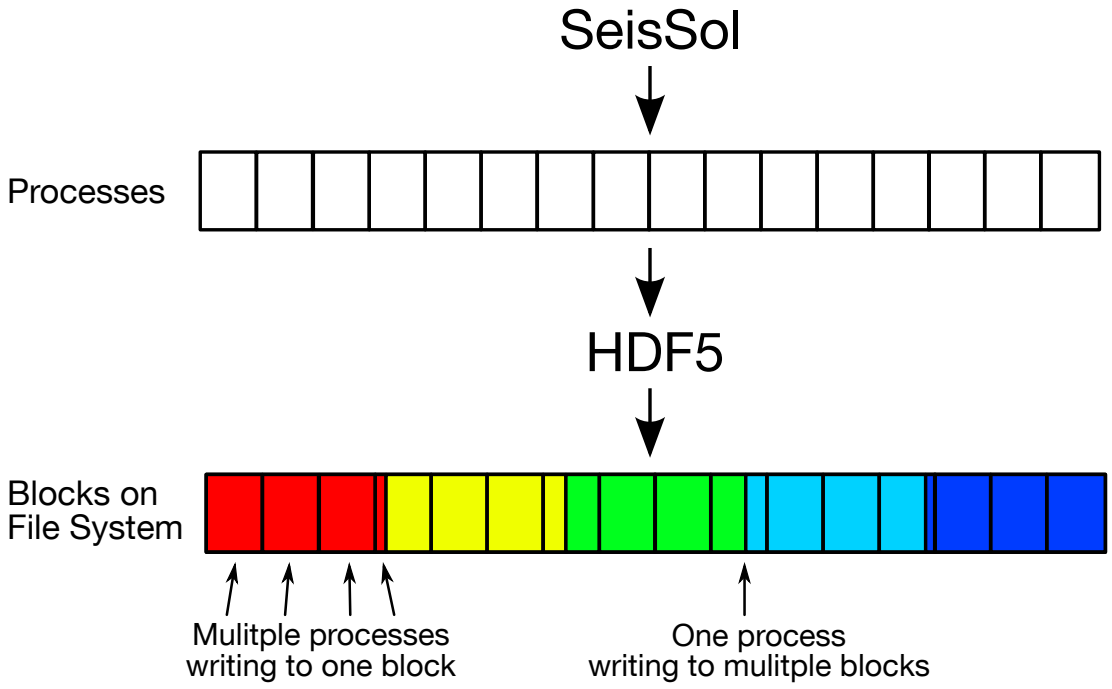

- SeisSol’s chunks are small ($\sim$ 200 KB per process) compared to the blocksize (8 MB on SuperMUC)
- thus: acquiring locks becomes the bottleneck

Aggregate and Align Data

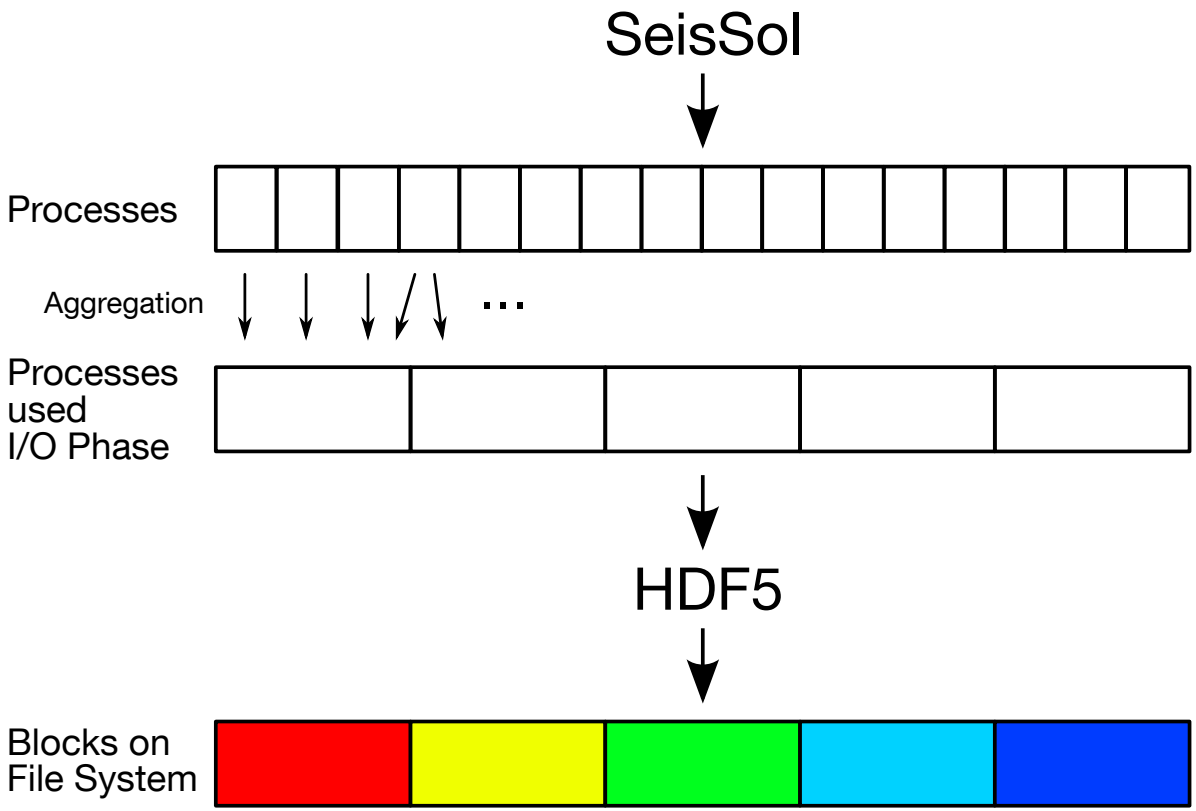

- Data is redistributed/aggregated to match file system blocks
- Not all processes may be included in the actual I/O phase

XDMF – First test application

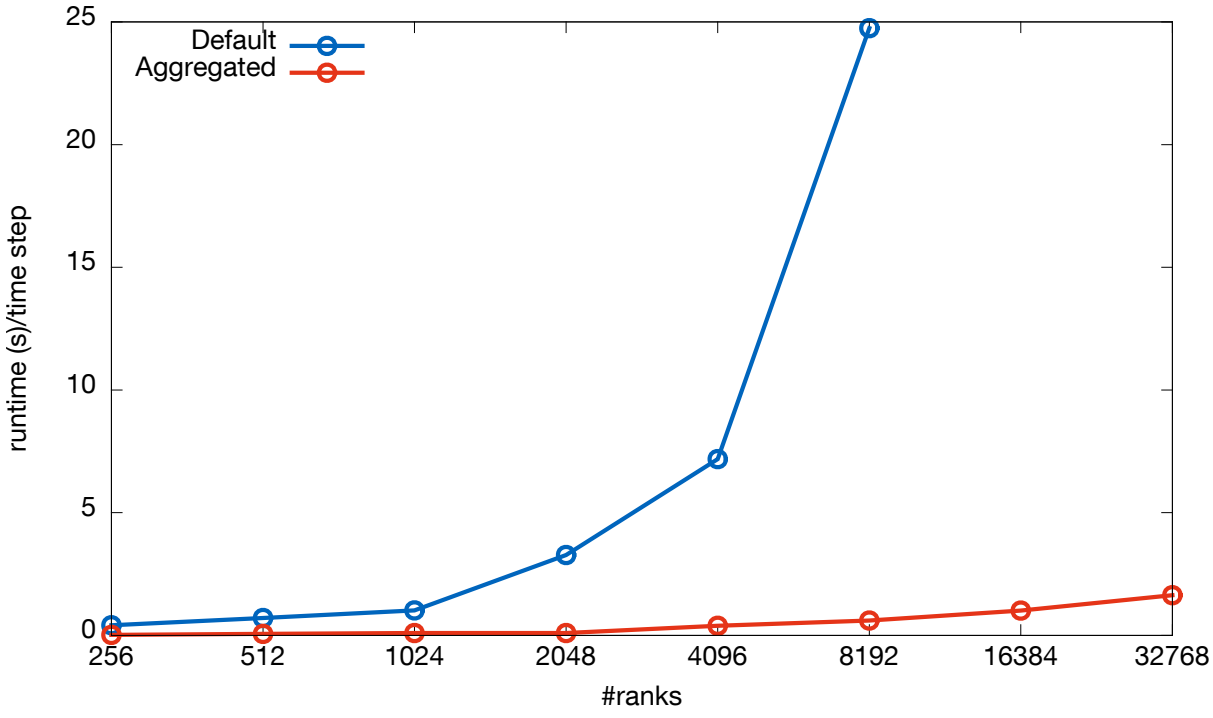

- $\sim 2 \times 78$ KB per process
  (simulates $\sim$10,000 elements with 2 variables per process)
- Exact element counts can vary ± 5 elements
  (simulates load imbalance from partitioners)
- SuperMUC: GPFS with 8 MB blocksize

Checkpointing - Latest results

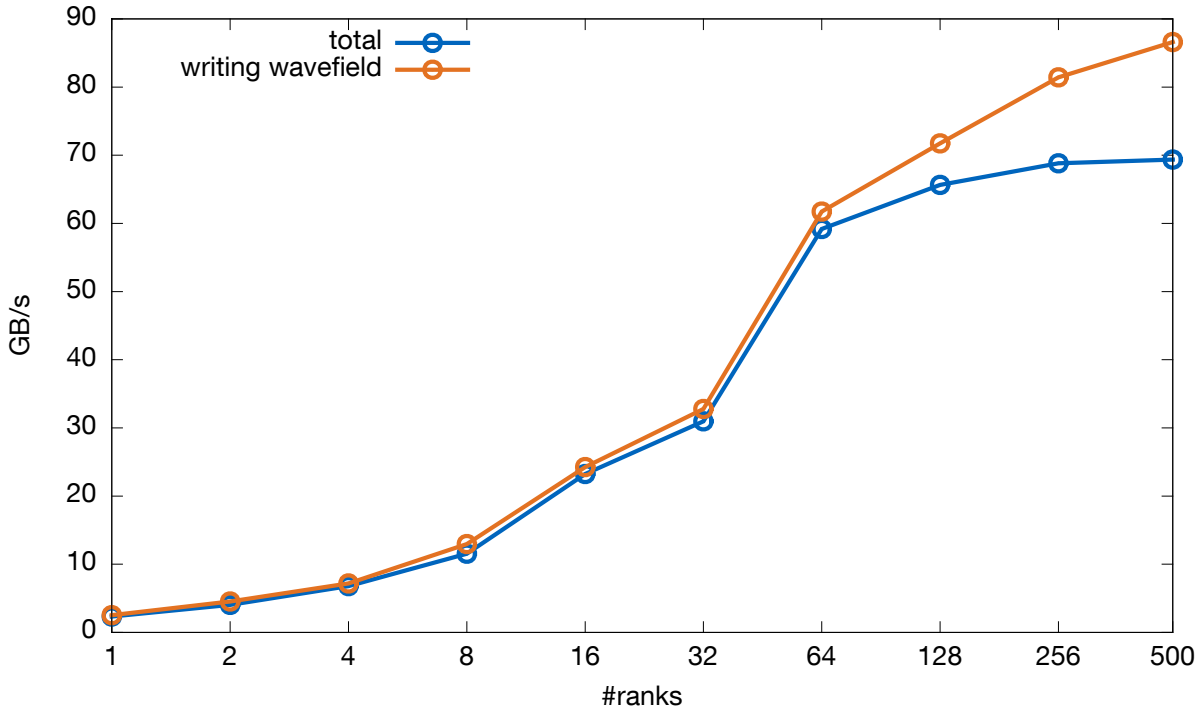

- Weak-scaling scenario with 640,000 elements per node, 6th order accuracy $\rightarrow$ Checkpoint size: 2.4 GB/node
- Total bandwidth includes additional overhead (writing metadata, flushing file, . . .)

Checkpointing - Latest results

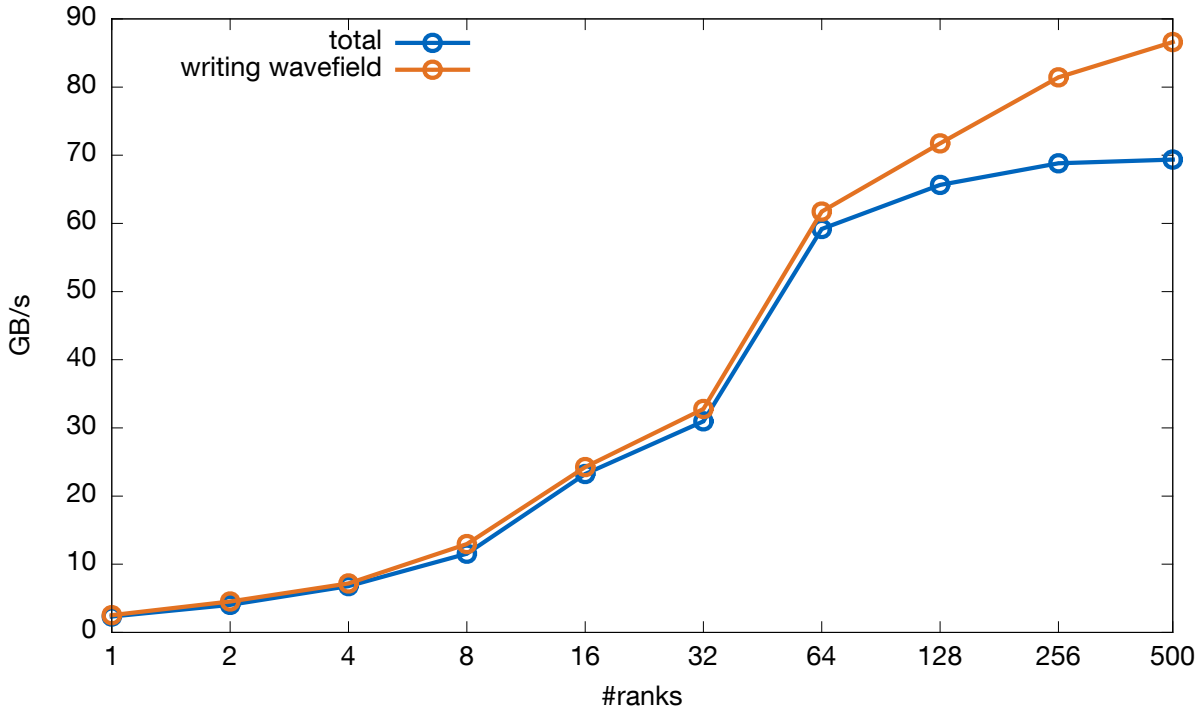

- GPFS on SuperMUC:
  Theoretical peak bandwidth on 9,216 nodes: 200 GB/s
- Overhead for writing a checkpoint every 1,000 timesteps is less than 0.5‰

Part III

Optimizing Kernel Operations in SeisSol

Breuer et al. [1,2]
PRACE ISC Award 2014

Seismic Wave Propagation with SeisSol

Elastic Wave Equations: (velocity-stress formulation)

$$q_t + Aq_x + Bq_y + Cq_z = 0$$

with $q = (\sigma_{11}, \sigma_{22}, \sigma_{33}, \sigma_{12}, \sigma_{23}, \sigma_{13}, u, v, w)^T$

$$A = \begin{pmatrix} 0 & 0 & 0 & 0 & 0 & 0 & -\lambda-2\mu & 0 & 0 \\ 0 & 0 & 0 & 0 & 0 & 0 & -\lambda & 0 & 0 \\ 0 & 0 & 0 & 0 & 0 & 0 & -\lambda & 0 & 0 \\ 0 & 0 & 0 & 0 & 0 & 0 & 0 & -\mu & 0 \\ 0 & 0 & 0 & 0 & 0 & 0 & 0 & 0 & 0 \\ 0 & 0 & 0 & 0 & 0 & 0 & 0 & 0 & -\mu \\ -\rho^{-1} & 0 & 0 & 0 & 0 & 0 & 0 & 0 & 0 \\ 0 & 0 & 0 & -\rho^{-1} & 0 & 0 & 0 & 0 & 0 \\ 0 & 0 & 0 & 0 & 0 & -\rho^{-1} & 0 & 0 & 0 \end{pmatrix} \quad B = \begin{pmatrix} 0 & 0 & 0 & 0 & 0 & 0 & 0 & -\lambda & 0 \\ 0 & 0 & 0 & 0 & 0 & 0 & 0 & -\lambda-2\mu & 0 \\ 0 & 0 & 0 & 0 & 0 & 0 & 0 & -\lambda & 0 \\ 0 & 0 & 0 & 0 & 0 & 0 & -\mu & 0 & 0 \\ 0 & 0 & 0 & 0 & 0 & 0 & 0 & 0 & -\mu \\ 0 & 0 & 0 & 0 & 0 & 0 & 0 & 0 & 0 \\ 0 & 0 & 0 & -\rho^{-1} & 0 & 0 & 0 & 0 & 0 \\ 0 & -\rho^{-1} & 0 & 0 & 0 & 0 & 0 & 0 & 0 \\ 0 & 0 & 0 & 0 & -\rho^{-1} & 0 & 0 & 0 & 0 \end{pmatrix}$$

- high order discontinuous Galerkin discretisation
- **ADER-DG**: high approximation order in space and time:
- additional features: local time stepping, high accuracy of earthquake faulting (full frictional sliding)

→ Dumbser, Käser et al. [4,6]

ADER-DG – Benefit of High Order

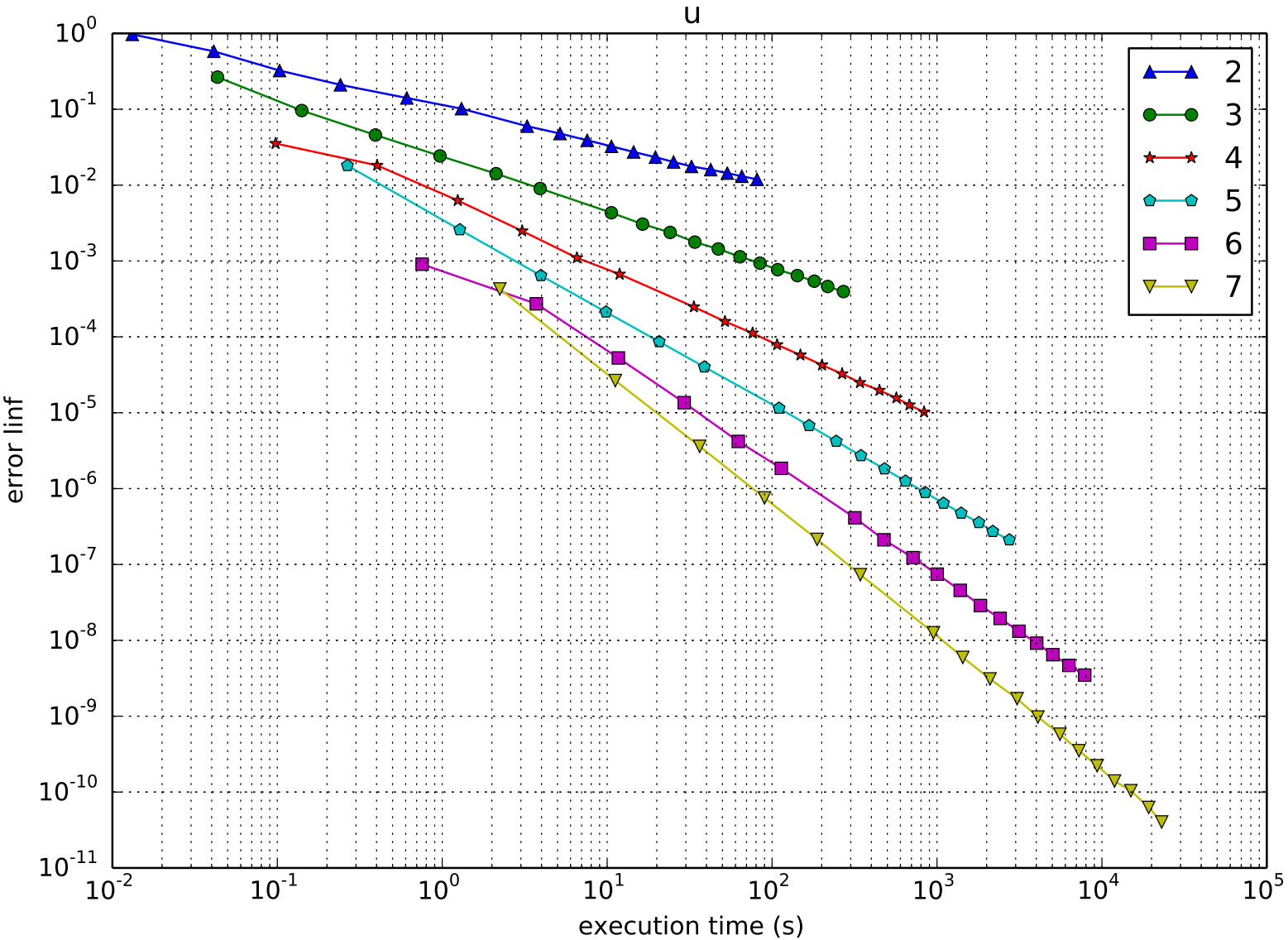

SeisSol in a Nutshell – ADER-DG

Update scheme

$$Q_k^{n+1} = Q_k - \frac{|S_k|}{|J_k|} M^{-1} \left(\sum_{i=1}^{4} F^{-,i} I(t^n, t^{n+1}, Q_k^n) N_{k,i} A_k^+ N_{k,i}^{-1} + \sum_{i=1}^{4} F^{+,i,j,h} I(t^n, t^{n+1}, Q_{k(i)}^n) N_{k,i} A_{k(i)}^- N_{k,i}^{-1} \right)$$
$$+ M^{-1} K^\xi I(t^n, t^{n+1}, Q_k^n) A_k^*$$
$$+ M^{-1} K^\eta I(t^n, t^{n+1}, Q_k^n) B_k^*$$
$$+ M^{-1} K^\zeta I(t^n, t^{n+1}, Q_k^n) C_k^*$$

Cauchy Kovalewski

$$I(t^n, t^{n+1}, Q_k^n) = \sum_{j=0}^{J} \frac{(t^{n+1} - t^n)^{j+1}}{(j+1)!} \frac{\partial^j}{\partial t^j} Q_k(t^n)$$

$$(Q_k)_t = -M^{-1} \left((K^\xi)^T Q_k A_k^* + (K^\eta)^T Q_k B_k^* + (K^\zeta)^T Q_k C_k^* \right)$$

Optimisation of Matrix Operations

Apply sparse matrices to multiple DOF-vectors Q_k

$$(K^{\xi})^T \qquad \frac{\partial^j}{\partial t^j} Q_k \qquad A_k^*$$

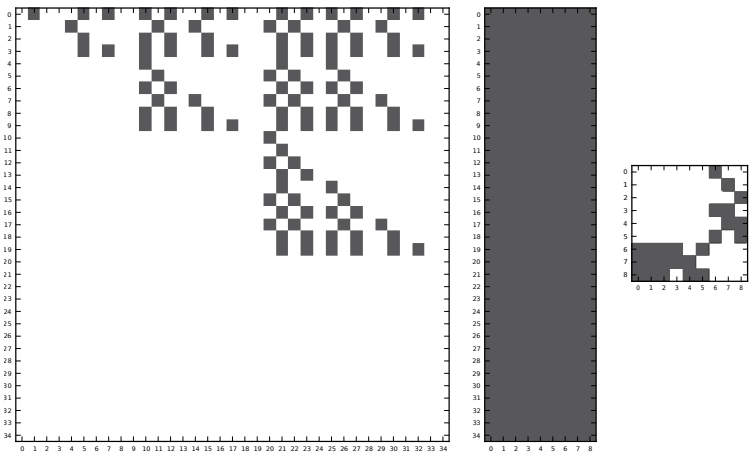

Code Generator for Sparse Kernels: (Breuer et al. [1])

- avoid overhead of CSR (or similar) data structures; store CSR elements vector, only
- full “unrolling” of all element operations using a code generator
- use intrinsics and apply blocking to improve vectorisation

Code Generator – Sparse Matrix Kernels

stiffness_matrices_3d.hpp

stiffness_matrices_3d.hpp › generatedMatrixMultiplication_kZetaT_3D_9_35(double* values, double* B, double* C)

```
#endif
#ifdef __SSE3__
__m128d b = _mm_loaddup_pd(&B[(i*35)+11]);
__m128d c11_0 = _mm_loadu_pd(&C[(i*35)+0]);
__m128d a11_0 = _mm_loadu_pd(&values[32]);
_mm_add_pd(c11_0, _mm_mul_pd(a11_0, b));
_mm_storeu_pd(&C[(i*35)+0], c11_0);
__m128d c11_2 = _mm_loadu_pd(&C[(i*35)+2]);
__m128d a11_2 = _mm_loadu_pd(&values[34]);
_mm_add_pd(c11_2, _mm_mul_pd(a11_2, b));
_mm_storeu_pd(&C[(i*35)+2], c11_2);
__m128d c11_4 = _mm_loadu_pd(&C[(i*35)+4]);
__m128d a11_4 = _mm_loadu_pd(&values[36]);
_mm_add_pd(c11_4, _mm_mul_pd(a11_4, b));
_mm_storeu_pd(&C[(i*35)+4], c11_4);
__m128d c11_6 = _mm_loadu_pd(&C[(i*35)+6]);
__m128d a11_6 = _mm_loadu_pd(&values[38]);
_mm_add_pd(c11_6, _mm_mul_pd(a11_6, b));
_mm_storeu_pd(&C[(i*35)+6], c11_6);
__m128d c11_8 = _mm_loadu_pd(&C[(i*35)+8]);
__m128d a11_8 = _mm_loadu_pd(&values[40]);
_mm_add_pd(c11_8, _mm_mul_pd(a11_8, b));
_mm_storeu_pd(&C[(i*35)+8], c11_8);
#else
C[(i*35)+0] += values[32] * B[(i*35)+11];
C[(i*35)+1] += values[33] * B[(i*35)+11];
C[(i*35)+2] += values[34] * B[(i*35)+11];
C[(i*35)+3] += values[35] * B[(i*35)+11];
```

Code Generator – Dense Kernels

dense_matrices.hpp

dense_matrices.hpp › generatedMatrixMultiplication_dense_56_9_56(double* A, double* B, double* C, double* A_prefetch = NULL, double* B_prefetch = NULL, double* C_prefetch = NULL)

```
inline void generatedMatrixMultiplication_dense_56_9_56(double* A, double* B, double* C, double* A_prefetch = NULL, double* B_prefetch = NULL
        , double* C_prefetch = NULL) {
//[...] SSE and AVX data types, SSE optimization
#if defined(__SSE3__) && defined(__AVX__)
//[...] pointers
for(int n = 0; n < 9; n+=3) {
  for(int m = 0; m < 48; m+=12) {
    //[...] pointers and loads
    for (int k = 0; k < 56; k++)
    {
    b_0 = _mm256_broadcast_sd(b0);
    //[...] more broadcasts and arithmetics on b
    a_0 = _mm256_load_pd(a0);
    a0+=4;
    c_0_0 = _mm256_add_pd(c_0_0, _mm256_mul_pd(a_0, b_0));
    c_0_1 = _mm256_add_pd(c_0_1, _mm256_mul_pd(a_0, b_1));
    c_0_2 = _mm256_add_pd(c_0_2, _mm256_mul_pd(a_0, b_2));
//[...] remaining kernel
#endif

#if defined(__MIC__)
//[...] MIC specifics
for(int n = 0; n < 9; n+=3) {
  //[...] MIC specifics
  #pragma prefetch b0,b1,b2,a0
  for(int k = 0; k < 56; k++)
  {
    //[...] MIC specifics
    c_0_0 = _mm512_fmadd_pd(a_0, b_0, c_0_0);
    c_0_1 = _mm512_fmadd_pd(a_0, b_1, c_0_1);
    c_0_2 = _mm512_fmadd_pd(a_0, b_2, c_0_2);
    a0 += 8;

//[...] remaining MIC kernel
#endif

#if !defined(__SSE3__) && !defined(__AVX__) && !defined(__MIC__)
//[...] fallback code
#endif

#ifndef NDEBUG
num_flops += 56448;
```

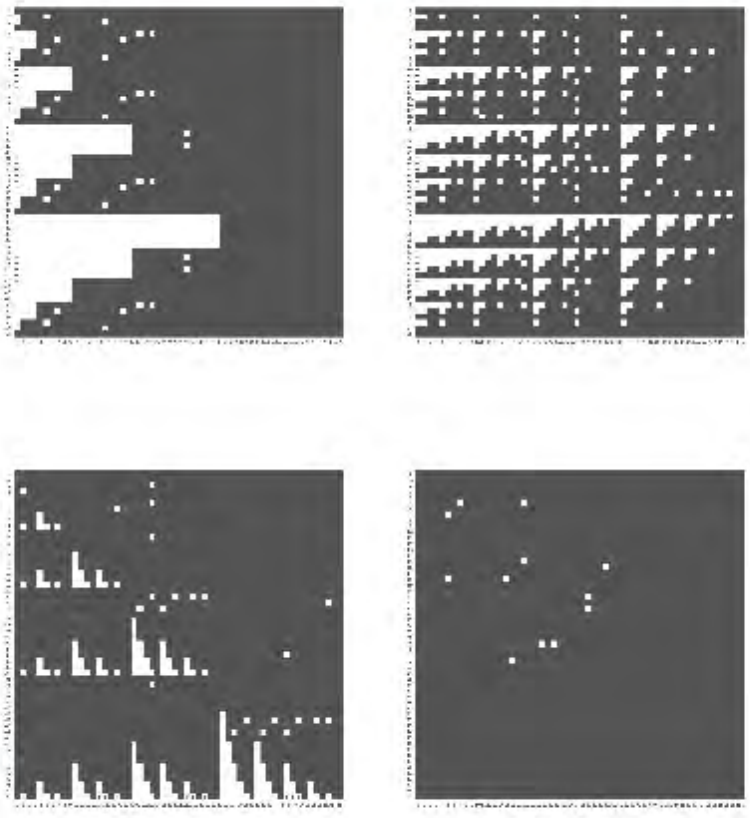

Optimisation of Matrix Operations

Apply sparse matrices to multiple DOF-vectors Q_k

$$\hat{K}^{\zeta} \quad Q_k^n \quad C_k^{\star} \qquad\qquad \hat{K}^{\zeta} \quad \frac{\partial^1}{\partial t^1} Q_k \quad C_k^{\star}$$

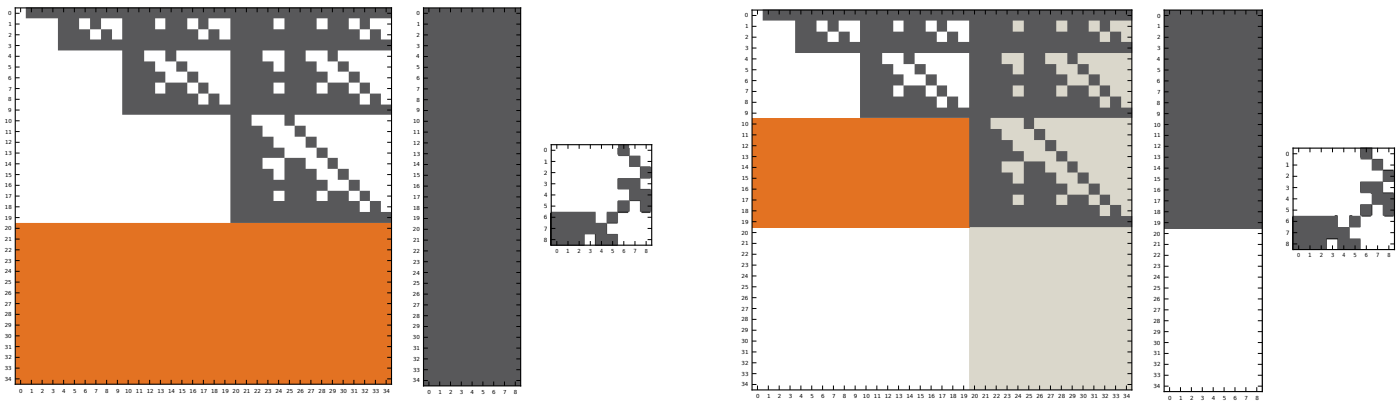

Dense vs. Sparse Kernels: (Breuer et al. [2])

- switch to dense kernels depending on achieved time to solution
- for sparse and dense kernels:
  exploit zero-blocks generated during recursive CK computation

Performance Optimization

Switch between Sparse/Dense Kernels:

- auto-tuning approach on benchmark scenarios
- measure sparse vs. dense performance for each matrix
- select sparse vs. dense kernel based on best time to solution

order							boundary
2	*sparse*	*sparse*	*sparse*	*sparse*	*sparse*	*sparse*	13%
3	*sparse*	*sparse*	*dense*	*sparse*	*sparse*	*sparse*	26%
4	*sparse*	*sparse*	*dense*	*sparse*	*dense*	*dense*	17%
5	*sparse*	*sparse*	*sparse*	*sparse*	*sparse*	*sparse*	23%
6	*sparse*	*dense*	*dense*	*sparse*	*dense*	*dense*	9%

Hybrid MPI+OpenMP Parallelisation:

- careful OpenMP parallelisation of all parts (not only main kernels $\rightarrow$ communication buffers, etc.)
- targeted at manycore platforms, such as Intel Xeon Phi
- OpenMP improvements for Xeon Phi also lead to noticeable improvements for “standard” CPUs

Part IV

Dynamic Rupture Simulation at Petascale – Xeon Phi Supercomputers

Heinecke et al.: *Petascale High Order Dynamic Rupture Earthquake Simulations on Heterogeneous Supercomputers* [3]
ACM Gordon Bell Finalist 2014

Supercomputing Platforms

SuperMUC @ LRZ, Munich

- 9216 compute nodes (18 “thin node” islands)
  147,456 Intel SNB-EP cores (2.7 GHz)
- Infiniband FDR10 interconnect (fat tree)
- #12 in Top 500: 2.897 PFlop/s

Stampede @ TACC, Austin

- 6400 compute nodes, **522,080 cores**
  2 SNB-EP (8c) + **1 Xeon Phi SE10P** per node
- Mellanox FDR 56 interconnect (fat tree)
- #7 in Top 500: 5.168 PFlop/s

Tianhe-2 @ NSCC, Guangzhou

- 8000 compute nodes used, **1.6 Mio cores**
  2 IVB-EP (12c) + **3 Xeon Phi 31S1P** per node
- TH2-Express custom interconnect
- #1 in Top 500: 33.862 PFlop/s

Optimization for Intel Xeon Phi Platforms

Offload Scheme:

- hides communication with Xeon Phi and between nodes
- use “heavy” CPU cores for dynamic rupture

Hybrid parallelism:

- on 1–3 Xeon Phis and host CPU(s)
- reflects multiphysics simulation
- manycore parallelism on Xeon Phi

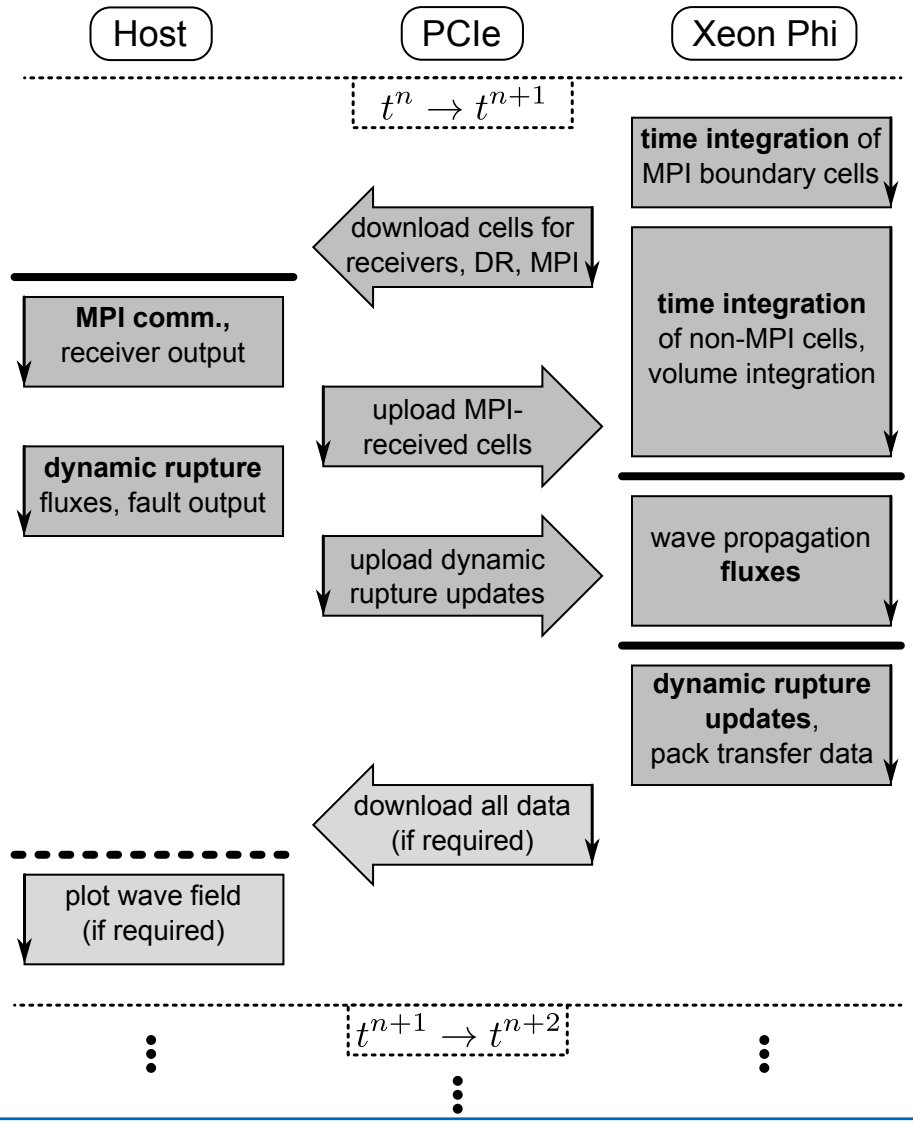

Weak Scaling of Wave Propagation

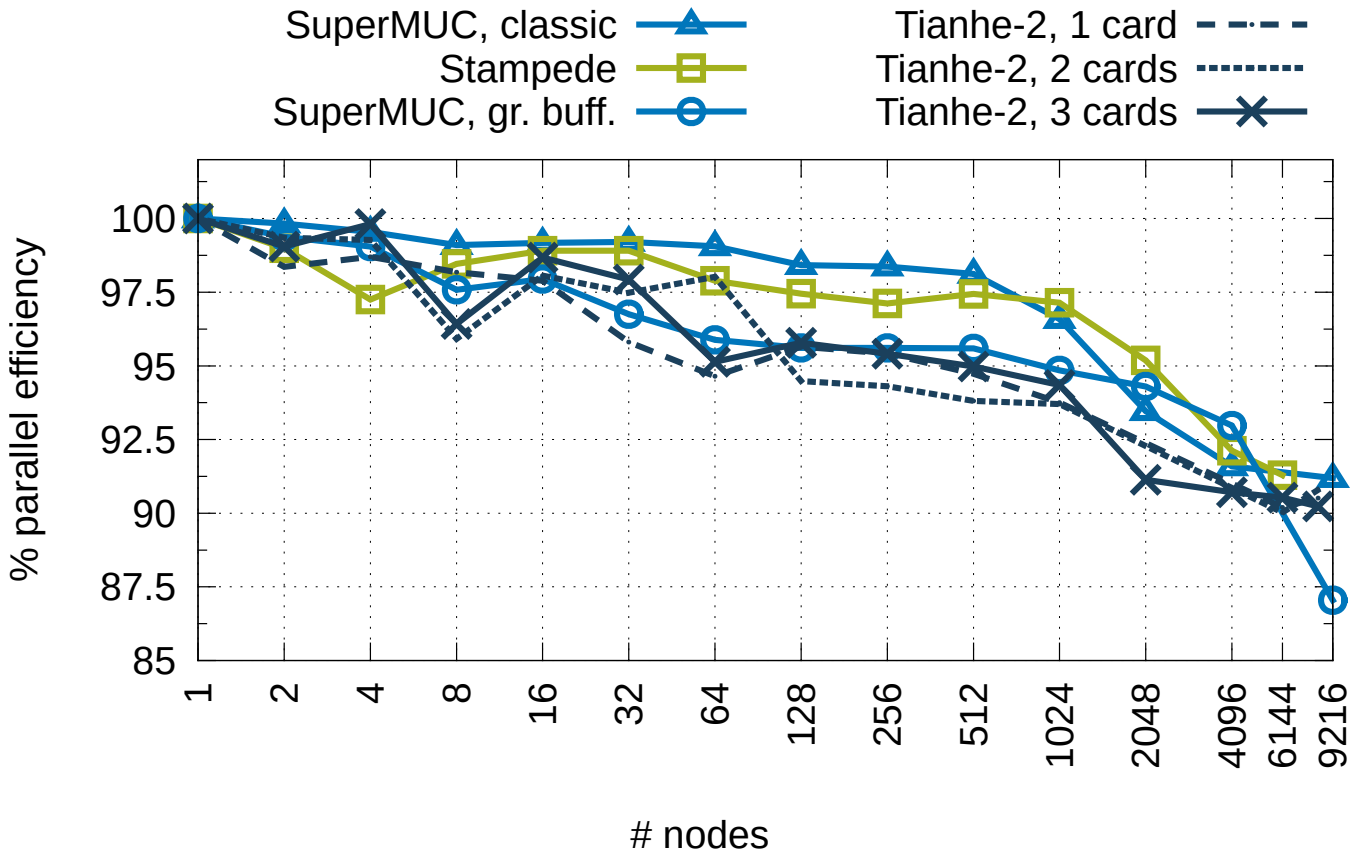

- goal: test scalability towards large problem sizes
- cubic domain, uniformly refined tetrahedral cells
- weak scaling: 400,000 elements per card/node

Weak Scaling of Wave Propagation

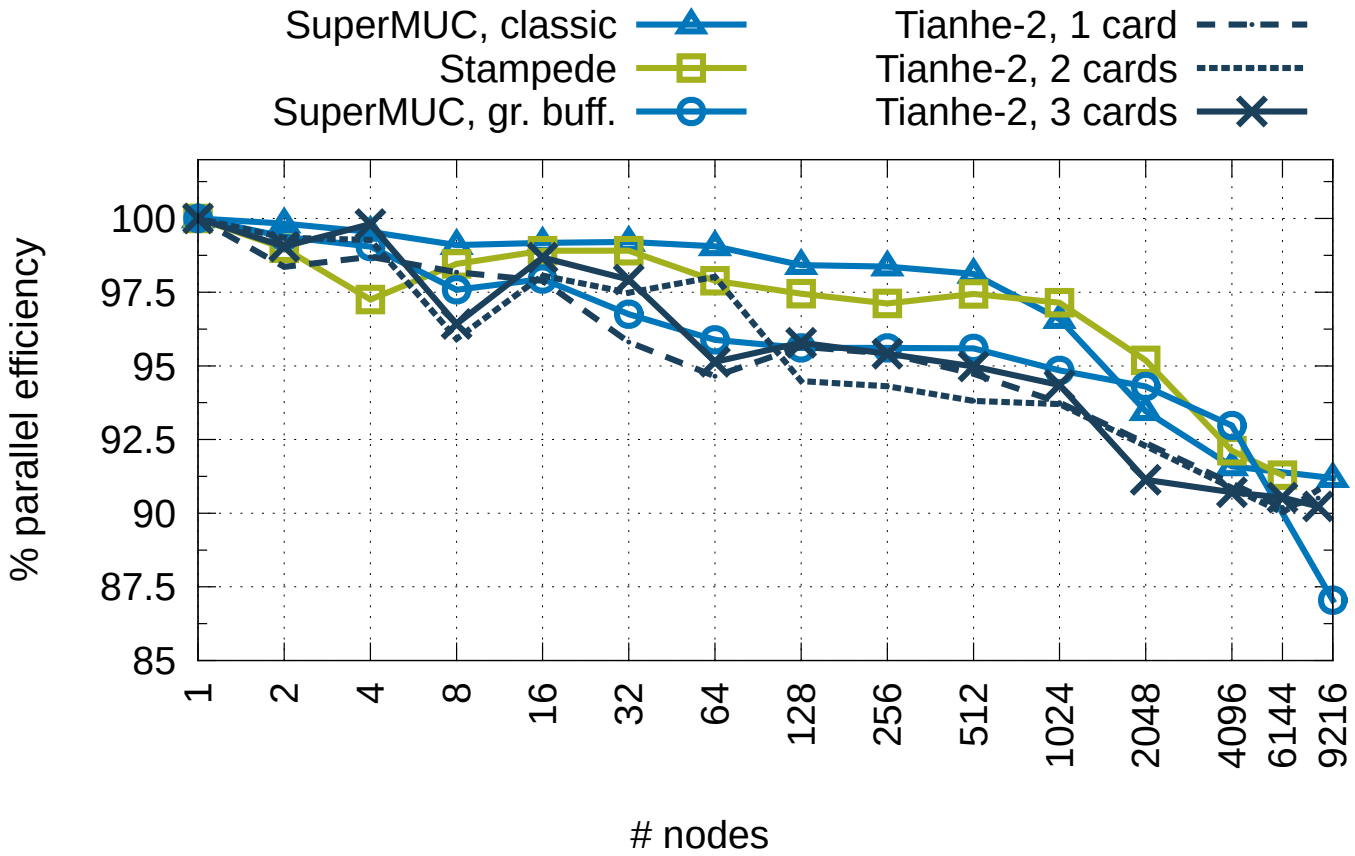

- more than 90 % parallel efficiency on Tianhe-2 and Stampede
- 87 % on full SuperMUC (no overlapping)

Weak Scaling of Wave Propagation

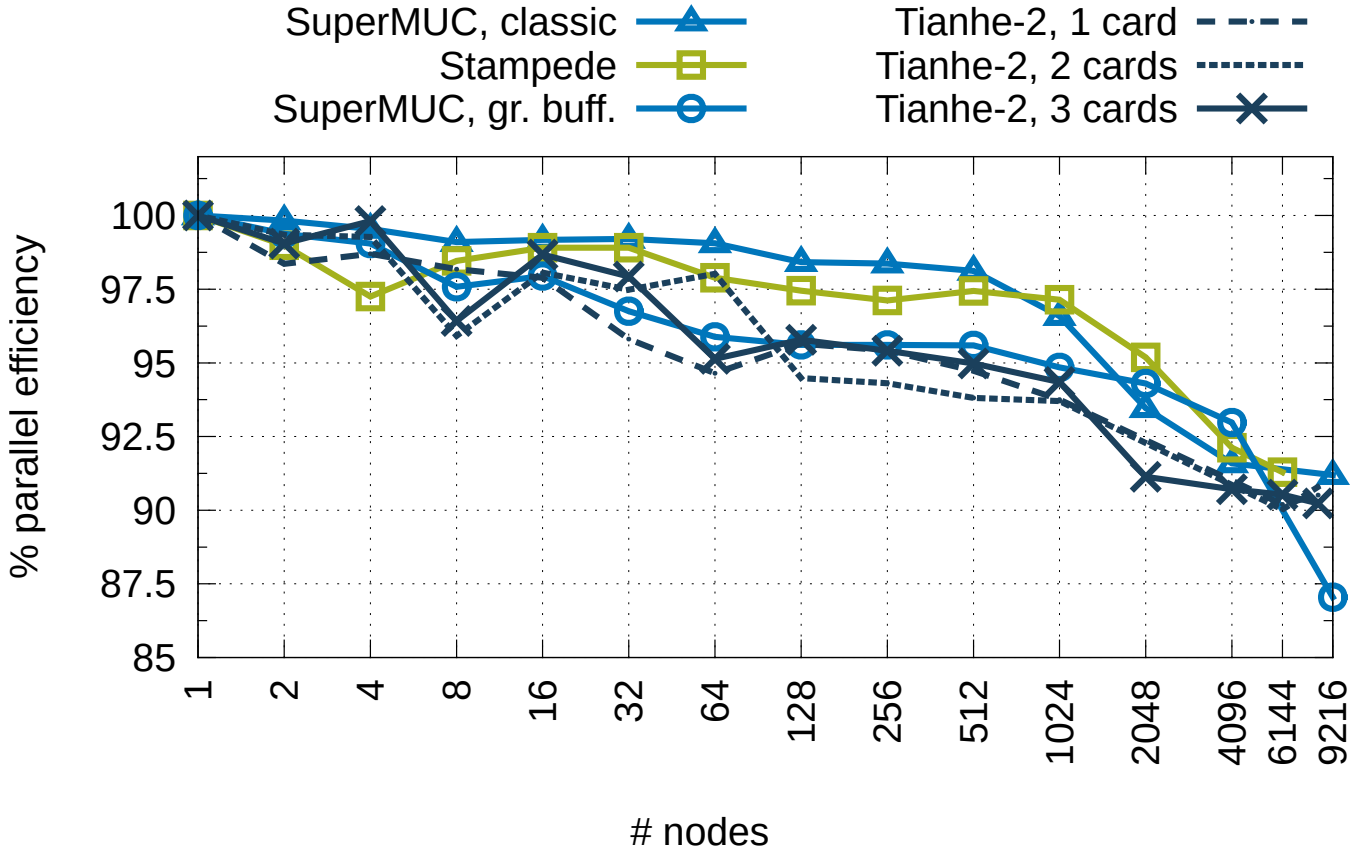

- 8.6 PFlop/s on Tianhe-2 (8000 nodes)
- 2.3 PFlop/s on Stampede (6144 nodes)
- 1.6 PFlop/s on SuperMUC (9216 nodes)

Weak Scaling – Peak Efficiency

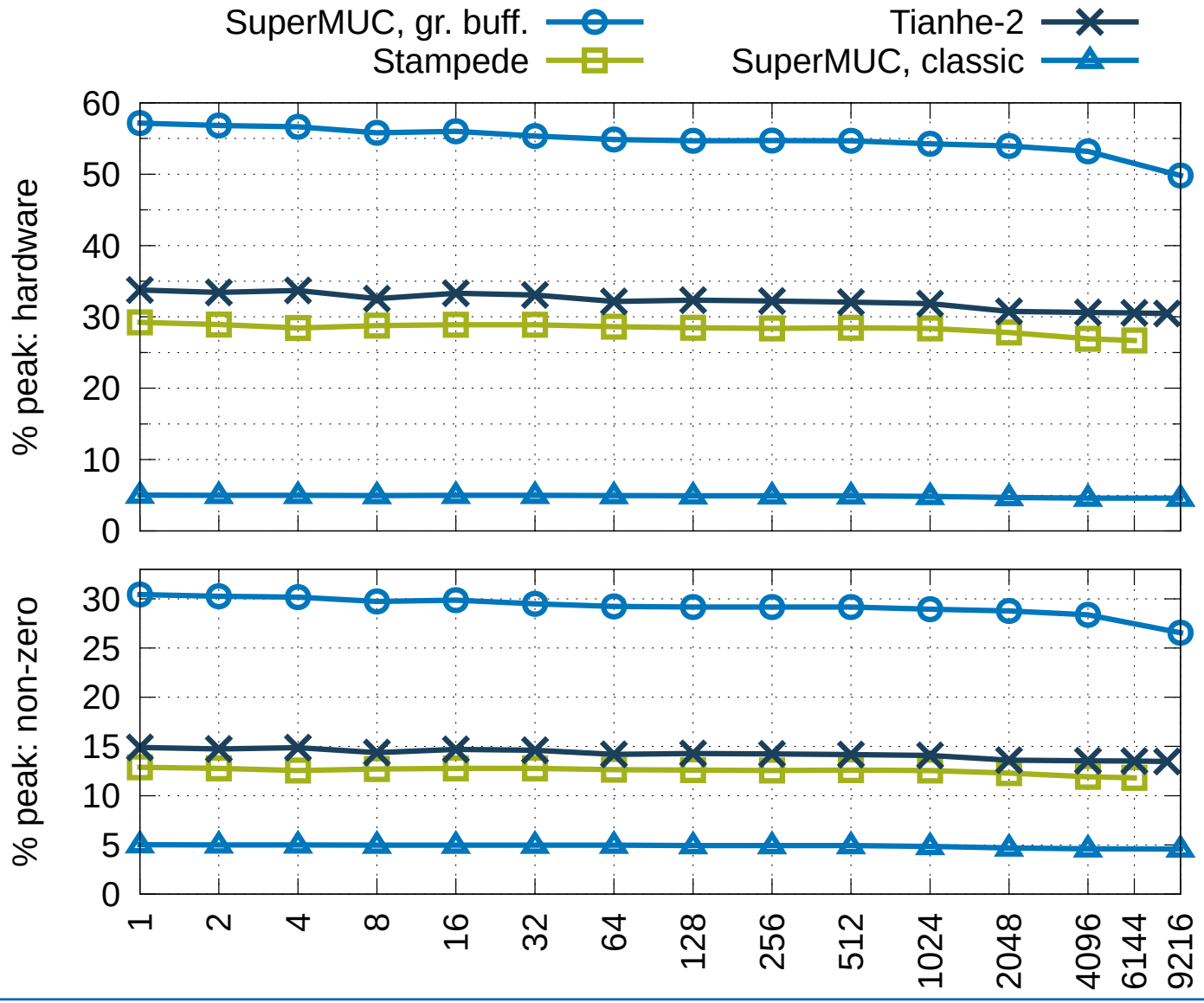

Strong Scaling of Landers Scenario

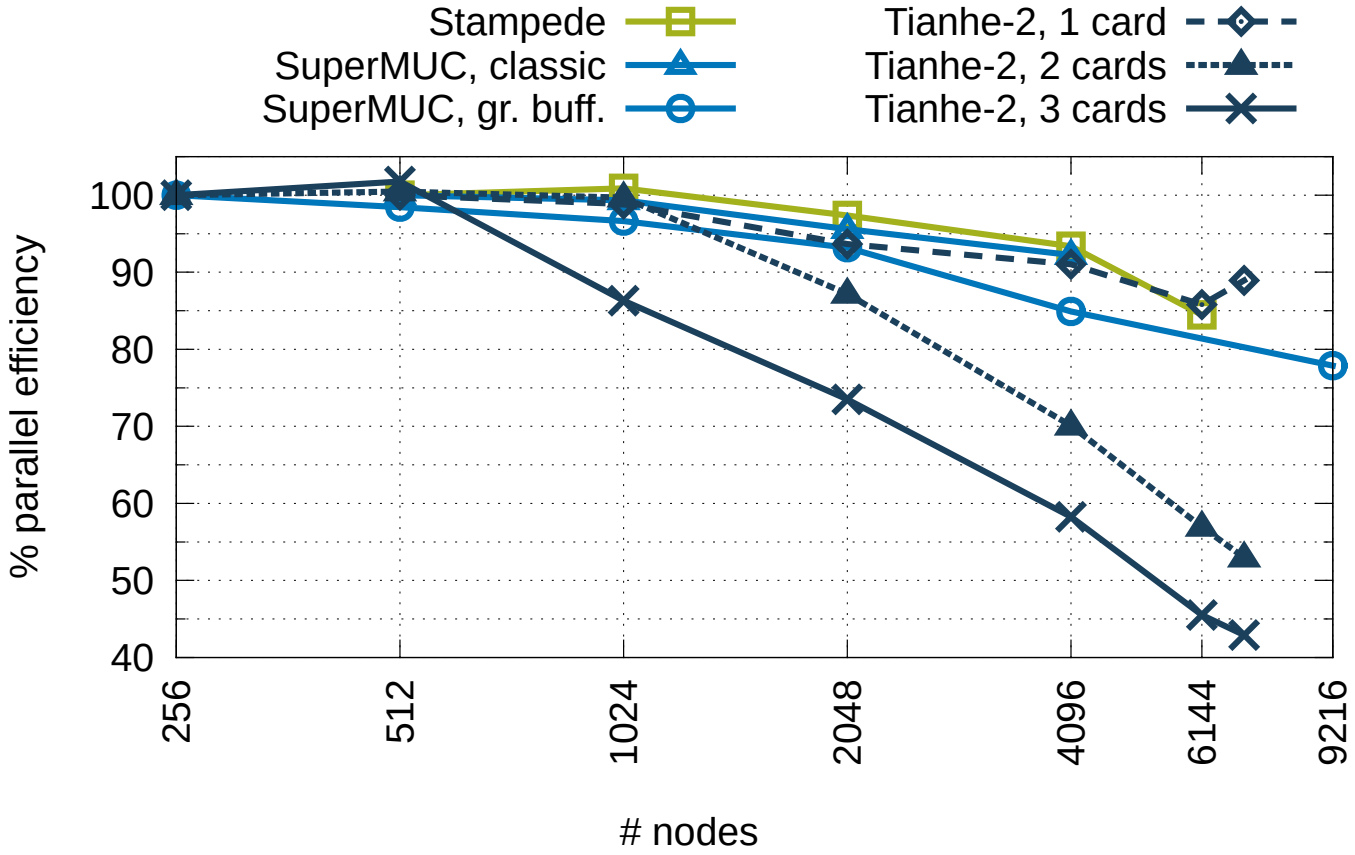

- 191 million tetrahedrons; 220,982 element faces on fault
- 6th order, 96 billion degrees of freedom

Strong Scaling of Landers Scenario

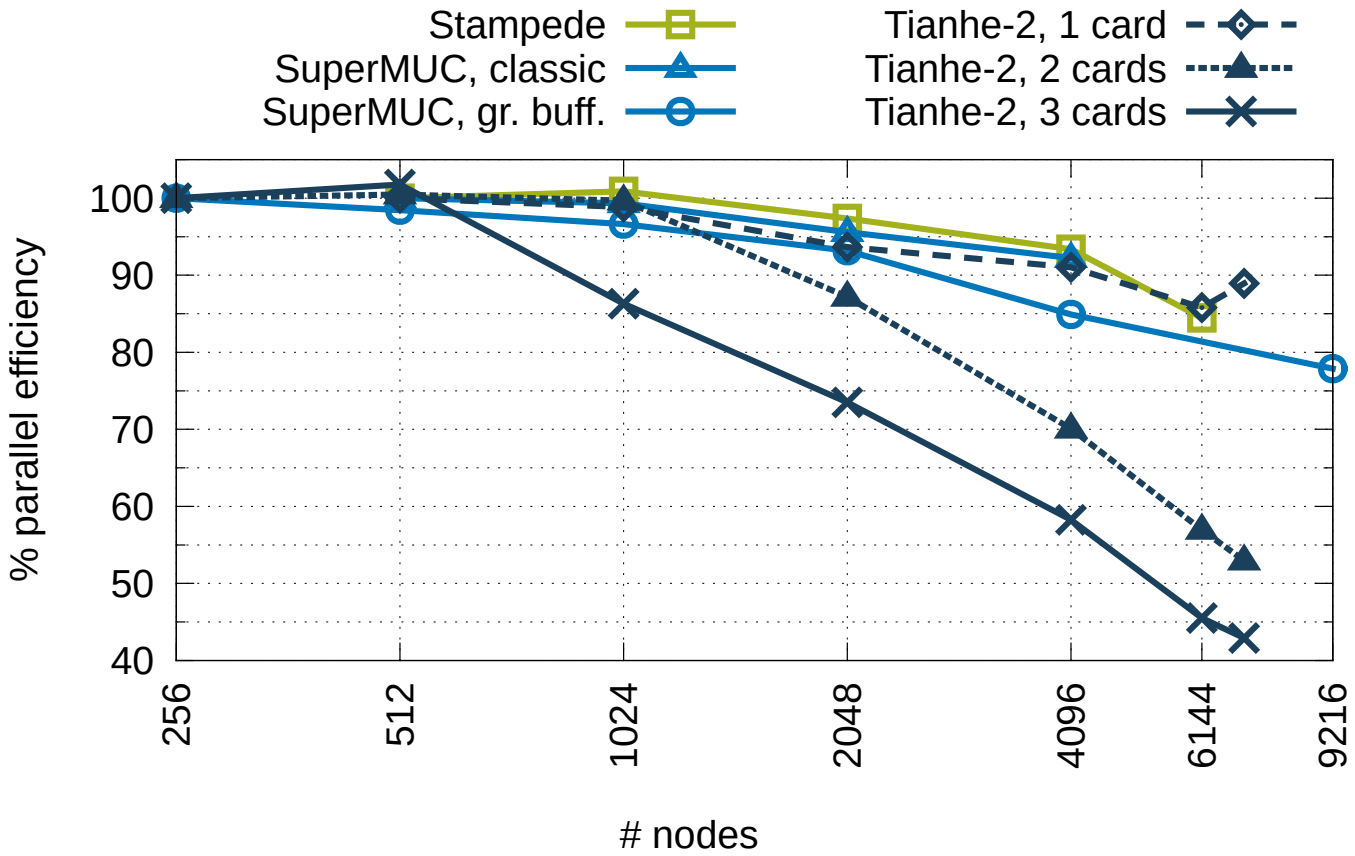

- more than 85 % parallel efficiency on Stampede and Tianhe-2 (when using only one Xeon Phi per node)
- multiple-Xeon-Phi performance suffers from MPI communication

Strong Scaling of Landers Scenario

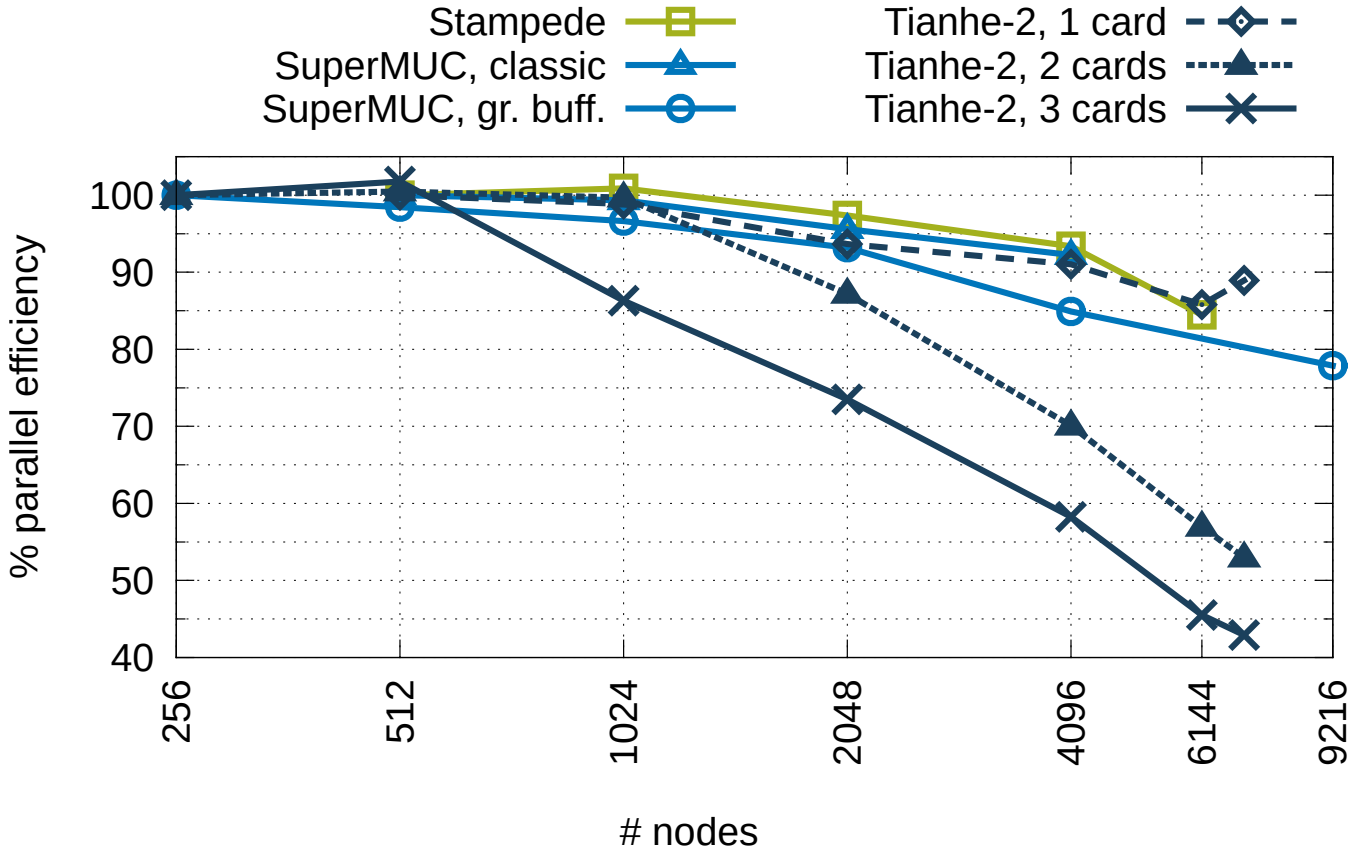

- 3.3 PFlop/s on Tianhe-2 (7000 nodes)
- 2.0 PFlop/s on Stampede (6144 nodes)
- 1.3 PFlop/s on SuperMUC (9216 nodes)

Landers Strong Scaling – Peak Efficiency

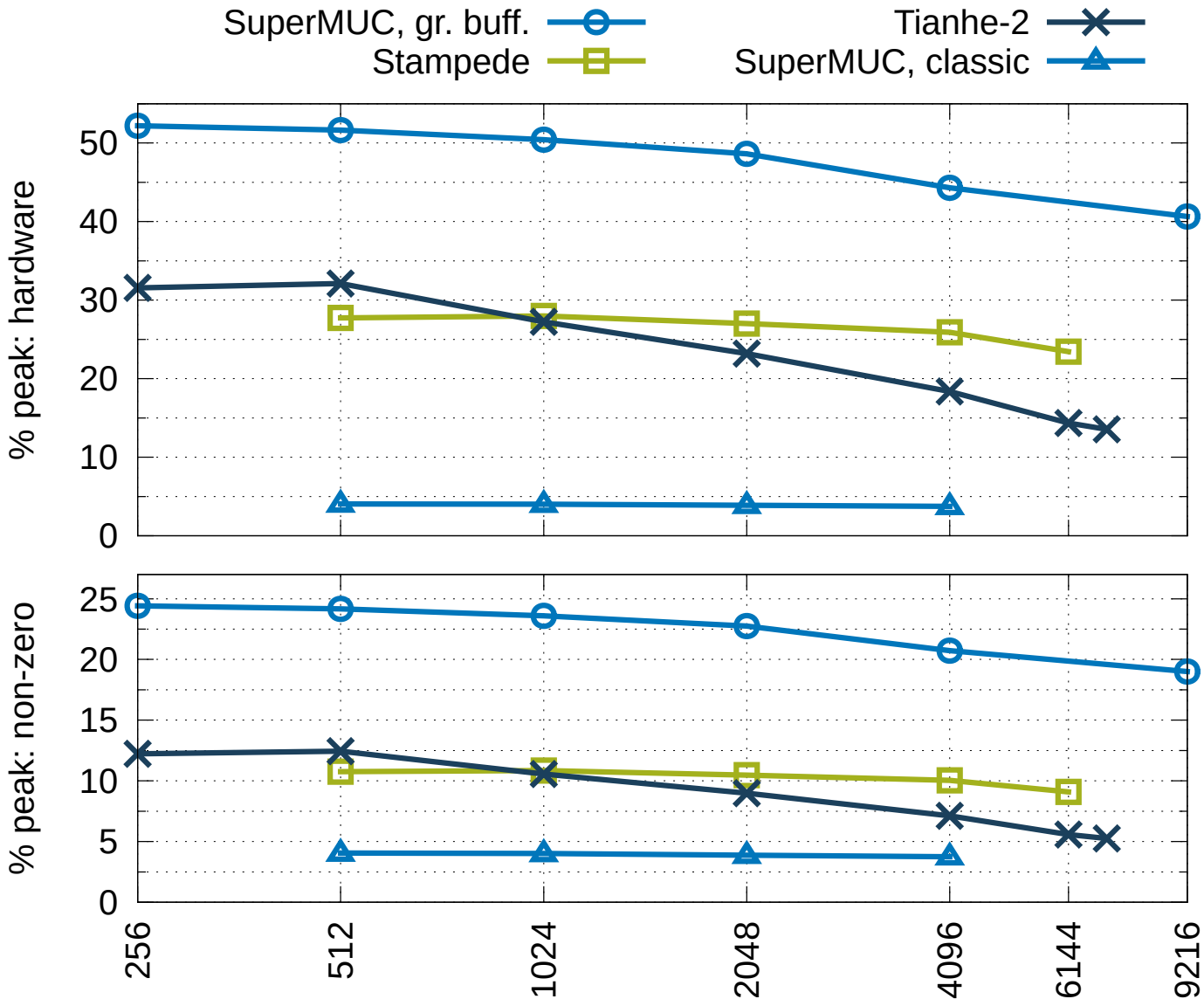

SeisSol: Latest/Current Work on Optimization

Further Performance Engineering:

- improved memory layout: separate ghost/copy layers, NUMA awareness
- alignment of data for matrix kernels (esp. important for MIC)
- overlap computation and communication (using more effective data layout)
- improved matrix kernels: assembler/machine code, AVX2 for Haswell

Towards Local Time Stepping:

- communication of time-integrated variables (instead of simple ghost cell exachange)
- more asychronous updates

SeisSol: Earthquake Simulation @ Petascale

Multiphysics Dynamic Rupture Simulations with SeisSol:

- high-order ADER-DG on complicated geometries
- non-linear interaction of rupture process and seismic waves
- physics-based seismic hazard analysis

Petascale Performance on Heterogeneous Platforms:

- scalable mesh input (and output) of more than 9 billion cells
- exploits high computational intensity of ADER-DG
- requires careful tuning of the entire simulation pipeline
- code generation to accelerate element kernels
- offload-scheme for multiphysics with Xeon Phi
- extreme (hybrid) parallelism with approx. 1.6 million cores

Acknowledgements

Special thanks go to . . .

- Intel:
  - Mikhail Smelyanskiy, Karthikeyan Vaidyanathan
  - Pradeep Dubey
- all colleagues from the three supercomputing centers, esp.:
  - Arndt Bode (Leibniz Supercomputing Centre)
  - William Barth (Texas Advanced Computing Centre)
  - Xiang-Ke Liao (NCSS and NUDT)
- for financial support:
  - Volkswagen Foundation (project ASCETE)
  - German Research Foundation
  - KONWIHR
- the entire SeisSol team and all contributors

References

[1] A. Breuer, A. Heinecke, M. Bader, C. Pelties: *Accelerating SeisSol by generating vectorized code for sparse matrix operators.* In: Advances in Parallel Computing 25, IOS Press, 2014. Proceedings of ParCo 2013

[2] A. Breuer, A. Heinecke, S. Rettenberger, M. Bader, A.-A. Gabriel, C. Pelties: *Sustained Petascale Performance of Seismic Simulations with SeisSol on SuperMUC.* In: Supercomputing, LNCS 8488, p. 1–18. PRACE ISC Award 2014.

[3] A. Heinecke, A. Breuer, S. Rettenberger, M. Bader, A.-A. Gabriel, C. Pelties, A. Bode, W. Barth, X.-K. Liao, K. Vaidyanathan, M. Smelyanskiy, P. Dubey: *Petascale High Order Dynamic Rupture Earthquake Simulations on Heterogeneous Supercomputers*. Gordon Bell Prize Finalist 2014.

[4] M. Dumbser, M. Käser: *An arbitrary high-order discontinuous Galerkin method for elastic waves on unstructured meshes – II. The three-dimensional isotropic case.* Geophys. J. Int. 167(1), 2006.

[5] P. Galvez, J-P. Ampuero, L.A. Dalguer, S. Somala, T. Nissen-Meyer: *Dynamic earthquake rupture modeled with an unstructured 3D spectral element method applied to the 2011 M9 Tohoku earthquake.* Geophys. J. Int., submitted.

[6] M. Käser, M. Dumbser, J. de la Puente, H. Igel: *An arbitrary high-order Discontinuous Galerkin method for elastic waves on unstructured meshes – III. Viscoelastic attenuation.* Geophys. J. Int. 168(1), 2007.